In Vivo Predictive Dissolution: Transport Analysis of the CO_2, Bicarbonate *In Vivo* Buffer System

BRIAN J. KRIEG,[1] SEYED MOHAMMAD TAGHAVI,[2] GORDON L. AMIDON,[1] GREGORY E. AMIDON[1]

[1]University of Michigan, College of Pharmacy, Ann Arbor, Michigan 48109
[2]McGill University, Department of Chemical Engineering, Montreal, Quebec H3A 2B2, Canada

Received 7 February 2014; revised 13 June 2014; accepted 14 July 2014

Published online 11 September 2014 in Wiley Online Library (wileyonlinelibrary.com). DOI 10.1002/jps.24108

ABSTRACT: Development of an oral *in vivo* predictive dissolution medium for acid drugs with a p*K*a in the physiological range (e.g., Biopharmaceutics Classification System Class IIa) requires transport analysis of the complex *in vivo* CO_2/bicarbonate buffering system. In this report, we analyze this buffer system using hydrodynamically defined rotating disk dissolution. Transport analysis of drug flux was predicted using the film model approach of Mooney et al[1] based on equilibrium assumptions as well as accounting for the slow hydration reaction, $CO_2 + H_2O \rightarrow H_2CO_3$. The accuracy of the models was compared with experimentally determined results using the rotating disk dissolution of ibuprofen, indomethacin, and ketoprofen. The equilibrium and slow hydration reaction rate models predict significantly different dissolution rates. The experimental results are more accurately predicted by accounting for the slow hydration reaction under a variety of pH and hydrodynamic conditions. Although the complex bicarbonate buffering system requires further consideration given its dynamic nature *in vivo*, a simplifying irreversible reaction (IRR) transport analysis accurately predicts *in vitro* rotating disk dissolution rates of several carboxylic acid drugs. This IRR transport model provides further insight into bicarbonate buffer and can be useful in developing more physiologically relevant buffer systems for dissolution testing. © 2014 Wiley Periodicals, Inc. and the American Pharmacists Association J Pharm Sci 103:3473–3490, 2014

Keywords: mathematical model; dissolution; transport; physicochemical; *in vitro* models; acid–base equilibria; diffusion

INTRODUCTION

When a drug product is administered orally, the absorption may be limited by the rate at which the drug dissolves in the gastrointestinal tract. For Biopharmaceutics Classification System Class II low solubility drugs, dissolution can be the rate-limiting step.[2] The composition of the intestinal fluid plays a critical role in determining this rate. One of the main components of intestinal fluid is the bicarbonate buffer species that controls lumenal pH. Buffers can have a large effect on the dissolution of ionizable drugs by affecting the pH at the solid liquid interface (surface) of the dissolving drug.[1,3–6]

Bicarbonate (HCO_3^-) is secreted by epithelial cells and the pancreas into the small intestine where it is the main buffer in the lumen and acts to maintain a relatively constant pH in the intestinal tract. Bicarbonate is thought to follow the Jacobs Stewart Cycle in the small intestine.[7–9] Bicarbonate (HCO_3^-) present in the intestinal lumen can react with hydrogen ions (H^+) to form carbonic acid (H_2CO_3), which then produces carbon dioxide [CO_2(aq)] and water (H_2O) through the dehydration reaction. This process is reversible (see Reaction 2 below) and carbon dioxide can diffuse into the intestinal cells or react with water to form carbonic acid through the hydration reaction. Carbonic acid can also ionize to form hydrogen ions and bicarbonate. In the intestinal cells, the same reversible process can occur, resulting in the formation of CO_2 (aq) and HCO_3^-. The HCO_3^- formed in the intestinal cells can be transported back into the intestinal lumen. The concentration of each of the species formed is dependent on the corresponding equilibrium constants.

Concentrations of aqueous carbon dioxide and bicarbonate are directly related in the luminal fluid of the GI tract.[10–12] In the stomach of healthy humans, the percent CO_2 typically ranges between 4% and 10% CO_2 (30–76 mmHg) and similar values are observed in the proximal jejunum.[12,13] McGeese and Hastings measured an average of 13.2% (100 mmHg) CO_2 in the jejunum at an average pH of 6.5.[14] In the proximal duodenum, where there is a lower pH, these values are typically significantly higher and can be as high as 66% CO_2 (500 mmHg).[15] These %CO_2 levels can be compared with normal atmospheric conditions, which are approximately 0.04%. The stomach secretes about 400 mmol of H^+ per day[9] (17 mmol/h), which enters the duodenum. Therefore, bicarbonate must be secreted at a rate in the duodenum that is high enough to neutralize the incoming H^+. This increase in bicarbonate and H^+ will result in an increase in the concentration of CO_2 partial pressure in the duodenum. Bicarbonate secretions have been shown to range from approximately 150–600 μmol cm^{-1} h^{-1} (~6 mmol/h) in the proximal duodenum to approximately 25–200 μmol cm^{-1} h^{-1} (~2 mmol/h) in the distal duodenum depending on the H^+ concentration.[11] The differences in the H^+ stomach secretions and duodenal bicarbonate secretions results in the pH of the proximal duodenum fluctuating up to 5 pH units transiently.[9]

An important consideration in more fully understanding the bicarbonate system are the individual reaction rates associated with the equilibrium constants K_c and K_{a1} in Reaction 2 below. In particular, the hydration and dehydration reactions associated with K_c are six to 10 orders of magnitude slower than the reaction rates associated with K_{a1}. The enzyme carbonic anhydrase is present in the intracellular fluid and membranes of the epithelial cells of the intestinal tract.[8,16] It functions

Correspondence to: Gregory E. Amidon (Telephone: 734-936-7438; Fax: 734-615-6162; E-mail: geamidon@umich.edu)

Journal of Pharmaceutical Sciences, Vol. 103, 3473–3490 (2014)
© 2014 Wiley Periodicals, Inc. and the American Pharmacists Association

to significantly accelerate the hydration and dehydration reactions in these regions. However, there is no evidence that carbonic anhydrase is secreted or present in the luminal fluid. Therefore, it is likely that the hydration and dehydration reactions occur at their slow rates in the bulk lumenal fluid.

Understanding the role of bicarbonate buffer and the reactions involved in its formation is essential to understanding the dissolution of weak acid and weak base drugs in the intestinal tract and, ultimately, to creating a more physiologically relevant dissolution medium. Although the impact that buffers have on a dissolving drug has been modeled accurately and is well understood, there has been little consideration of the effect of bicarbonate buffer on drug dissolution in the intestine.[1,3–6] There have been several studies characterizing the effect bicarbonate buffer has on drug dissolution and attempts have been made at modeling the process.[5,10,17–19] However, a thorough examination of how the CO_2 reaction chemistry of bicarbonate buffer affects drug dissolution has not been explored, although this is an area that has been studied rigorously and applied in geology and other sciences.[20–24] It is anticipated that a better understanding of the impact of bicarbonate buffer on the pH at the surface of a dissolving ionizable drug will provide the foundation for creating buffer systems that more closely resemble *in vivo* conditions and dissolution.

The significant role the slow hydration and dehydration rates have on the formation of bicarbonate and its ability to function as a buffer and alter the pH at the surface of dissolving drug (i.e., at the solid liquid interface) has been investigated in this study. The simultaneous convective diffusion and chemical reaction within the boundary layer model assuming either: (a) instantaneous chemical equilibrium, or (b) slow hydration and dehydration will be compared with experimental results using the defined hydrodynamics of the rotating disk dissolution system for weak acid drugs. Our analysis and experimental results demonstrate that the slow irreversible reaction rate (IRR) model best matches the experimental rotating disk dissolution rate of the weak acid drugs studied. This analysis can be helpful in developing buffering systems that are more physiologically relevant for *in vivo* dissolution predictions and testing. A similar analysis may be applied to weak base and amphoteric drugs. We have successfully applied this approach to weak base drugs and is the subject of a future publication.

Reactions and Kinetics of the Bicarbonate Buffer System

Conversion of CO_2(g) to CO_2(aq)

Bicarbonate buffer can be produced experimentally by controlling the partial pressure of CO_2 (g) equilibrated with water as shown in reactions 1 and 2.

$$CO_2(g) \overset{K_H}{\rightleftarrows} CO_2\,(aq) \qquad \text{(Reaction 1)}$$

$$CO_2\,(aq) + H_2O \overset{K_c}{\rightleftarrows} H_2CO_3 \overset{K_{al}}{\rightleftarrows} H^+ + HCO_3^- \qquad \text{(Reaction 2)}$$

The concentration of carbon dioxide dissolved in water, CO_2 (aq), follows Henry's Law constant (K_H) and the partial pressure of carbon dioxide gas [$P_{CO_2(g)}$].

$$K_H = \frac{CO_2\,(aq)}{P_{CO_2}\,(g)} \qquad (1)$$

Table 1. Measured Values from Literature and Estimated Values of Henry's Law Constant for Carbon Dioxide at Different Temperature and Ionic Strength

Solvent	Temperature (°C)	Henry's Law Constant
Water	35	0.027 (Ref. 26)
Water	40	0.024 (Ref. 26)
0.2 M NaCl Solution	35	0.026 (Ref. 26)
0.2 M NaCl Solution	40	0.023 (Ref. 26)
Isotonic solution (0.0154 M)	37	0.024[a]

[a]Estimated using the van't Hoff Equation for temperature dependence and ionic strength dependence from Butler.[25]

The solubility of carbon dioxide in water decreases as the temperature and ionic strength increases[25] and K_H may be adjusted to account for physiologically relevant conditions (37°C, isotonic solution, $K_H = 0.024$). This value is in close agreement with experimental values shown in Table 1.

The Reversible Reaction Between CO_2(aq) and H_2O(1) to Form H_2CO_3 (Hydration and Dehydration Reactions)

Reaction 2 is composed of two separate steps and the equilibrium constants of each reaction (K_c and K_{a1}) govern the overall reaction. The reaction of CO_2 (aq) with water to form H_2CO_3 is given by:

$$CO_2\,(aq) + H_2O \overset{K_c}{\leftarrow} H_2CO_3 \qquad \text{(Reaction 3)}$$

The value for K_c is equal to the ratio for the hydration rate of CO_2 (aq) and the dehydration rate of H_2CO_3.

$$K_c = \frac{k_h}{k_d} \qquad (2)$$

$$K_c = \frac{[H_2CO_3]}{[CO_2\,(aq)]} \qquad (3)$$

The hydration (k_h) and dehydration rate constants (k_d) vary with temperature and ionic strength. Values obtained experimentally in the range of 30°C–40°C are shown in Table 2. The reaction rate values are approximately ~0.1–0.16 s^{-1} for the hydration rate and ~50–80 s^{-1} for the dehydration rate. These reactions rates are very slow (e.g., 10^6 to 10^{10} times slower) relative to typical ionization reaction rates that are considered to be instantaneous as discussed below.

The Reversible Ionization of H_2CO_3 to form HCO_3^- and H^+

The value for K_{a1} shown in Reaction 2 is composed of the forward reaction rate (k_{a1f}) for the ionization of carbonic acid to form HCO_3^- and H^+ and the reverse reaction rate (k_{a1r}) where HCO_3^- reacts with H^+ to form H_2CO_3.

$$H_2CO_3 \overset{K_{al}}{\rightleftarrows} H^+ + HCO_3^- \qquad \text{(Reaction 4)}$$

$$K_{a1} = \frac{k_{a1f}}{k_{a1r}} \qquad (4)$$

Table 2. Experimental Values from Literature Obtained for the Hydration and Dehydration Rate Constant of Carbonic Acid, Carbon Dioxide, and Water

Temperature (°C)	Solvent	K_h (s^{-1})	K_d (s^{-1})
38	Buffer mixture with gaseous CO_2	0.161 (Ref. 27)	
40	Water	0.143 (Ref. 28)	
38	Phosphate buffer	0.062 (Ref. 29)	
37	Imidazole buffer with CO_2 gas or sodium bicarbonate	0.145 (Ref. 30)	49.5 (Ref. 30)
32.5	HCl and sodium bicarbonate mixture (made to ionic strength of 0.65 with NaCl)	0.057 (Ref. 31)	50.2 (Ref. 31)
36.7	HCl and sodium bicarbonate mixture		80 (Ref. 32)
36.9	HCl and sodium bicarbonate mixture		49.04 (Ref. 33)
37	HCl and potassium bicarbonate mixture (0.1 M ionic strength)		72 (Ref. 34)

$$K_{a1} = \frac{[H^+][HCO_3^-]}{[H_2CO_3]} \tag{5}$$

The value of K_{a1} depends on temperature and ionic strength. Table 3 presents experimental values of pKa ~ 3.55 reported at approximately 37°C. Information regarding exact values for the forward and reverse ionization rates at 37°C is limited. However, values for the reaction rate constants determined by Eigen and Hammes[35] at 25°C were s^{-1} and $k_{a1r} = 4.7 \times 10^{10} s^{-1}$. These values are 6–10 orders of magnitude greater than the hydration (k_h) and dehydration rate (k_d) constants described above. It can be assumed that Reaction 4 occurs instantaneously compared with rates of diffusion.

The Overall Equilibrium Reaction Constant K_a

It is often assumed that the entire reaction (Reaction 2) is at equilibrium where K_c and K_{a1} are combined to give an overall K_a value (Eqs. (6a) and (6b)) and Reaction 2 is simplified to Reaction 5.

$$CO_2 + H_2O \overset{K_a}{\rightleftarrows} HCO_3^- + H^+ \qquad \text{(Reaction 5)}$$

$$K_a = \frac{[H_2CO_3]}{[CO_2\,(aq)]} \cdot \frac{[H^+][HCO_3^-]}{[H_2CO_3]} = \frac{[H^+][HCO_3^-]}{[CO_2\,(aq)]} \tag{6a}$$

$$K_a = \frac{[H^+][HCO_3^-]}{[CO_2\,(aq)]} \tag{6b}$$

K_a has been determined at different temperatures and ionic strengths to be pKa ~6. Using experimentally obtained data as shown in Table 4, it is possible to adjust K_a based on temperature and ionic strength.

When assuming equilibrium, Eq. (6b) can be rearranged to calculate the bicarbonate concentration in solution as a function of dissolved carbon dioxide [$CO_{2(aq)}$] and pH:

$$[HCO_3^-] = \frac{K_a\,[CO_2\,(aq)]}{[H^+]} \tag{7}$$

Alternatively, this can be written as a function of the partial pressure of carbon dioxide (P_{CO_2}) using K_H, assuming

Table 3. Experimental Values from Literature Obtained at Different Experimental Conditions for the Equilibrium Constant K_{a1} (Ratio of the Forward and Reverse Ionization Reaction)

Temperature (°C)	Solvent	K_{a1}	pKa$_1$
35	Buffer with NaCl (ionic strength = 0.143)	2.816×10^{-4} (Ref. 36)	3.55
35	Aqueous solution	1.67×10^{-4} (Ref. 37)	3.78
38	Aqueous solution	1.59×10^{-4} (Ref. 37)	3.80

Table 4. Experimental Values from Literature Obtained at Different Experimental Conditions for the Overall Equilibrium Reaction Constant K_a

Temperature (°C)	Solvent	pKa
35	Aqueous solution	6.31 (Ref. 26)
35	Aqueous solution	6.31 (Ref. 38)
35	Aqueous solution made to ionic strength 0.1 with NaCl	6.07 (Ref. 38)
35	Aqueous solution made to ionic strength 0.2 with NaCl	6.01 (Ref. 38)
40	Aqueous solution	6.30 (Ref. 26)
40	Aqueous solution made to ionic strength 0.1 with NaCl	6.05 (Ref. 38)
40	Aqueous solution made to ionic strength 0.2 with NaCl	6.00 (Ref. 38)
38	Phosphate buffer with sodium bicarbonate (ionic strength = 0.12)	6.09 (Ref. 39)
32.5	HCl and sodium bicarbonate mixture (made to ionic strength of 0.65 with NaCl)	5.94 (Ref. 31)
37	Isotonic solution (ionic strength = 0.154)	6.05 calculated

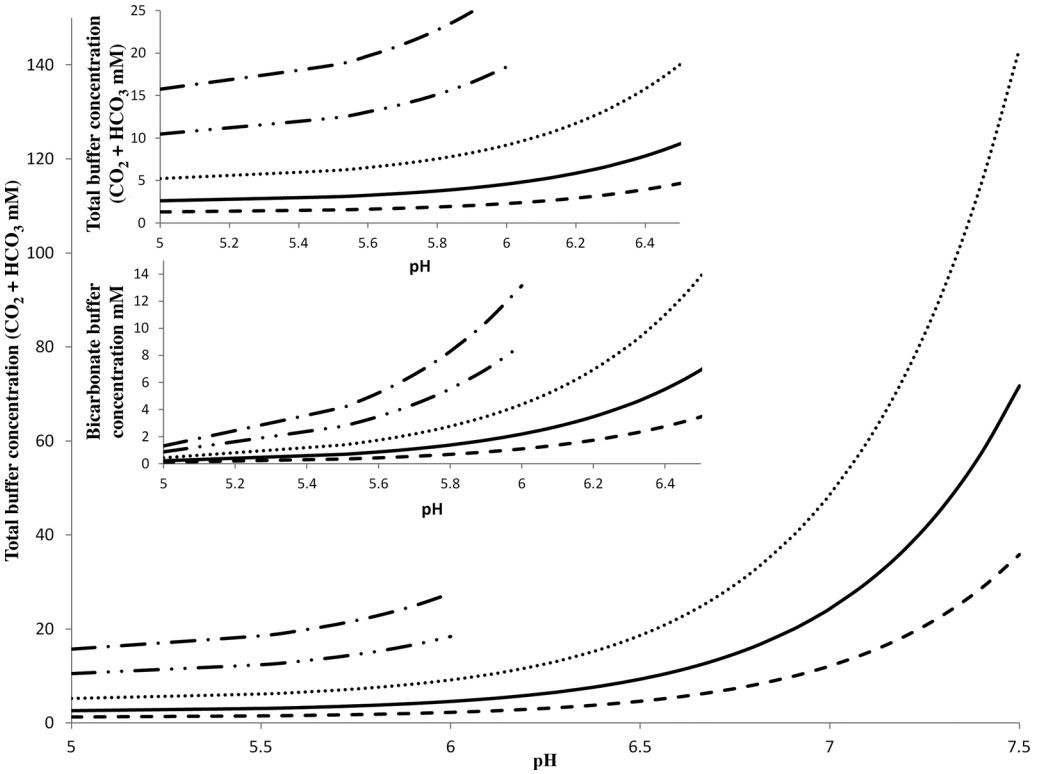

Figure 1. Total buffer and bicarbonate buffer concentrations (mM) at physiologically relevant pH values as function of %CO_2 in the solution (100% = 1 atm) at 37°C. Key (▬ ▬ ▬) 5% CO_2; (▬▬▬) 10% CO_2; (.....) 20% CO_2; (▬ ▪) 40% CO_2; (▬ ▪ ▪) 60% CO_2.

equilibrium.

$$[HCO_3^-] = \frac{K_a K_H P_{CO_2}}{[H^+]} \tag{8}$$

The values for P_{CO_2} and $[H^+]$ can be adjusted to yield a desired bicarbonate buffer concentration. At low pH values, the total buffer concentration, when CO_2 (aq) concentration is included, is relatively high due to high CO_2 (g) partial pressures found *in vivo* in the duodenum. Because of the solubility limitations of carbon dioxide and the effect of $[H^+]$ on the concentration of bicarbonate, the presence of bicarbonate is most significant for pH values in the range: $5.5 \leq pH \leq 7.5$. For pH below 5.5, only very dilute bicarbonate buffer concentrations can be produced even at high CO_2 (g) partial pressures. At pH values above 7.5, only low CO_2(g) values are required to achieve relevant bicarbonate buffer concentrations though the buffer capacity is substantially reduced. The relationship between CO_2 (g), CO_2 (aq), $[H^+]$, and $[HCO_3^-]$ is shown in Figure 1. Typical physiologic conditions of pH and carbon dioxide levels result in total buffer concentrations (CO_2(aq) + $[HCO_3^-]$) in the duodenum and jejunum in the range of 3–20 mM as shown in Figure 1. Figure 1 also compares the total buffer concentration to the bicarbonate concentration as a function of pH. The bicarbonate concentration present is significantly less than the total buffer concentration especially at low pH values.

Simultaneous Diffusion and Reaction Model

Dissolution of drugs from a solid surface are generally accurately predicted by considering the simultaneous diffusion and chemical reactions as described by Mooney et al.[1,40] Applying this to a rotating disk dissolution apparatus permits the estimation of pH at the surface of a compacted drug by taking into account the properties of the drug and buffer system and assuming simultaneous and instantaneous diffusion and chemical reaction in the hydrodynamic boundary layer near the surface of the rotating disk. Levich characterized this boundary layer thickness for a rotating disk based on liquid viscosity, rotational speed, and diffusion coefficient[41,42]:

$$h = 1.61 D^{1/3} \omega^{-1/2} \upsilon^{1/6} \tag{9}$$

When the Levich theory is applied to rotating disk drug dissolution, h is the thickness of the diffusion layer, D is the diffusion coefficient of the drug in the dissolving medium (aqueous buffer), υ is the kinematic viscosity (at 37°C water = 0.007 cm^2/s), and ω is the rotational speed (100 rpm = 10.47 radians/s). The diffusion layer thickness is a constant for each specific drug under fixed conditions of rotational speed (see Table 5). Following Mooney et al.,[1] the simultaneous

Table 5. The Effect Diffusion Layer Thickness (Ibuprofen Used for h Calculation) has on the Time CO_2 Spends in the Diffusion Layer (t_D) and How it Compares with the Reaction Time (t_r = *6.25* s)

h (μm)	t_D	t_r/t_D
61 (50 rpm)	0.76	8.2
43 (100 rpm)	0.38	16
27 (250 rpm)	0.15	42
19 (500 rpm)	0.076	82
14 (1000 rpm)	0.04	156

diffusion and chemical reaction model assuming instantaneous reaction was applied to the bicarbonate buffer system.

Applying a Simultaneous Diffusion and Reaction Model to Bicarbonate Buffer

The reaction rate for the hydration of carbon dioxide to carbonic acid is a slow process as described above. If the time the diffusing molecule spends in the diffusion layer is less than the reaction time, then the reaction would primarily be occurring only in the bulk solution and not in the diffusion layer.[43] The average residence time of a molecule in the diffusion layer is determined by diffusion layer thickness and the diffusivity of the molecule[43] (Eq. (10)). The reaction time depends on the first order rate constant and it defines the time needed for the reaction to be 63% complete[43] (Eq. (11)). Equations (10) and (11) can be used to assess the extent that a reaction will go to completion within the diffusion layer:

$$t_{\mathrm{D}} = \frac{h^2}{2D_{\mathrm{i}}} = \frac{1.3v^{1/3}}{D_{\mathrm{i}}^{1/3}w} \tag{10}$$

where t_{D} is the average residence time of a diffusing molecule in the diffusion layer. The reaction time, t_{r}, is given by Eq. (11) where k is the first order rate constant.

$$t_{\mathrm{r}} = \frac{1}{k} \tag{11}$$

If the hydration reaction between CO_2 (aq) and H_2O does not occur sufficiently fast, the reaction will not go to completion in the diffusion layer and the flux of bicarbonate throughout the diffusion layer will be less than predicted. Table 5 compares the ratio of t_{r} ($\sim$6.25 s^{-1}) and t_{D} at different diffusion layer thickness values (based on ibuprofen) calculated at different rotational speeds. These values were calculated according to the Levich equation for boundary layer thickness at the surface of a rotating disk (Eq. (9)). The table shows that $t_{\mathrm{r}} > t_{\mathrm{D}}$ even at large diffusion layer thickness values (low rpm) and that t_{r} can vary between an order of magnitude to two orders of magnitude greater than t_{D}. This analysis indicates that the hydration reaction is occurring to a very limited extent in the diffusion layer, whereas the dehydration reaction appears sufficiently fast that it may be assumed to be occurring rapidly enough that these difference in reaction rates will impact the buffer capacity of bicarbonate in the diffusion layer. It is worth noting that these differences are relevant in the diffusion layer but not in the bulk aqueous phase where all the reactions occur sufficiently fast to be considered instantaneous and Reaction 5 and K_a apply.

As the results will show, this slow reaction has a large effect on the experimental flux in comparison with predictions applying the instantaneous reaction film model[1] to bicarbonate buffer. Initially, two different chemical equilibrium approaches were applied. The first approach was to assume that all of the reactions in the formation of bicarbonate buffer are sufficiently fast so that the chemical equilibrium that is assumed to occur in the bulk solution (and displayed in Reaction 5) can be applied to the boundary layer in the film model [pKa = 6.04; bulk chemical equilibrium (BCE) model]. When applying the BCE model, CO_2 is the nonionized form of the buffer and HCO_3^- is the ionized form of the buffer. The second approach assumed that both the hydration reaction and dehydration reaction are so slow in comparison with the ionization reactions that the formation of bicarbonate is dependent only on Reaction 4 [pKa$_1$ = 3.55, carbonic acid ionization (CAI) model]. In the case of the CAI model, H_2CO_3 is the nonionized form of the buffer and HCO_3^- is the ionized form. It is notable that the concentration of CO_2(aq) is 300 times greater than carbonic acid. Therefore, the total buffer concentration used in the CAI model is less than that used in the BCE model, which includes the CO_2 (aq) concentration. However, the results show that these two assumptions do not accurately describe experimental results. Therefore, a modification to the transport analysis that incorporates the slow reaction rates for the hydration and dehydration reactions is necessary.

Incorporating Reaction Rates into a Simultaneous Diffusion and Chemical Reaction Model

The experimental results (see below) indicate that when reactions occur non-instantaneously, the film model needs to account for the slow reactions. There are multiple species reacting in the diffusion layer during the dissolution of a weak acid or weak base drug, which makes adding reaction rates into the film model challenging. Therefore, to follow the same steps using the simultaneous diffusion and chemical reaction model, two assumptions were made to simplify the process. The first assumption is that only the hydration and dehydration reaction rates need to be considered and all other reactions can be assumed to take place instantaneously. The second assumption is that since the hydration reaction (k_{h}) happens very slowly, it can be assumed to not be taking place at all in the diffusion layer (although it will occur in the bulk) and the only reaction rate that needs to be included in the modeling process is the dehydration reaction rate (k_{d}). These assumptions describe a situation where the protons formed at the surface of the dissolving weak acid drug will react with HCO_3^- to form H_2CO_3, which can then form CO_2 and H_2O through an irreversible chemical reaction (irreversible reaction model, IRR). This assumption, when applied to the film model changes the resulting equation for calculating the surface pH and the total buffer concentration does not include CO_2 concentration. The surface pH is no longer independent of reaction rates and diffusion layer thickness because the dehydration reaction rate and diffusion layer thickness remain included in the equation for surface pH. The experimental results show that using the irreversible reaction model (IRR model) allows for accurate predictions of drug flux in bicarbonate buffer. The derivation of the IRR model is presented in the appendix and the cubic equation needed to solve for surface pH and drug flux are shown in Appendix Eqs. (A34) and (A35d).

MATERIALS AND METHODS

Ibuprofen (Albermarle - Baton Rouge, Louisiana, USA U; Lot#11550–0005), indomethacin (Alexis Biochemicals - San Diego, California USA; ≥98%, Lot#L25666, and ketoprofen (Sigma–Aldrich - St. Louis Missouri, USA; Lot#044K0790) were used as received and all other chemicals used were of analytical grade. Distilled water was used for all experiments. Mineral oil United States Pharmacopeia (USP) grade was used for the titration experiment to prevent the escape of CO_2(g). All dissolution runs were performed in a jacketed beaker at 37°C. Two runs were done for each experimental condition described

Table 6. Drug and Buffer Properties Applied to the Simultaneous Diffusion and Reaction Model

Species	Solubility (M)	p*K*a	Diffusion Coefficient (cm^2/s)
Ibuprofen	3.30×10^{-4} (Ref. 44)	4.43 (Ref. 44)	7.93×10^{-6a}
Indomethacin	5.963×10^{-6b}	4.27 (Ref. 45)	6.8×10^{-6} (Ref. 46)
Ketoprofen	5.303×10^{-4b}	4.02 (Refs.47)	9.3×10^{-6} (Ref. 5)
Bulk bicarbonate		6.04^b	14.6×10^{-6} (Ref. 48)
Carbonic acid		3.55 (Ref. 11)	14.6×10^{-6} (Ref.48)
Carbon dioxide	0.02403		24.9×10^{-6} (Ref. 49)

[a]Estimated using the Wilke–Chang equation.
[b]Measured experimentally.
Other values were taken from literature.

below. Samples were analyzed using a UV spectrophotometer (Agilent Technologies - Santa Clara, California, USA; Model# 61103A). The samples were obtained using a flow through system that recycled the analyzed solution back into the dissolution vessel. The standard curves were also made using the UV flow through system.

Ibuprofen solubility was measured by agitating a suspension of ibuprofen particles in 50 mM acetate buffer at pH 4.5 while being kept at 37°C. The pH of the saturated solution at 37°C was measured to be 4.5. Samples were taken from the solutions and filtered before they were diluted with 50 mM acetate buffer at pH 4.5. The measured solubility was 0.150 mg/mL and based on the pH-solubility profile this solubility is in good agreement with an intrinsic solubility of 0.068 mg/mL used in this paper and reported by Karl et al.[44]

The intrinsic solubility of indomethacin was measured by agitating a suspension of indomethacin particles in 0.1 N hydrochloric acid solution while being kept at 37°C. Samples were taken from the solutions and filtered before they were diluted with 0.1 N hydrochloric acid.

The intrinsic solubility of ketoprofen was measured by agitating a suspension of ketoprofen particles in 0.1 N hydrochloric acid solution while being kept at 37°C. Samples were taken from the solutions and filtered before they were diluted with pH 6.7 25 mM phosphate buffer.

The p*K*a of the bicarbonate buffer was measured by adjusting 100% dry compressed air and 100% carbon dioxide (at appropriate ratios to give physiologically relevant conditions) in a 100 mL 0.9%NaCl solution in a jacketed beaker at 37°C. Solid NaOH and a 5 N NaOH solution were used to adjust the buffer pH to ~7.0. Next, the sources of the gas mixture were eliminated from the solution and USP grade mineral oil (heated to 37°C) was added to the buffer solution where it produced an oil layer on top of the aqueous buffer to limit the escape of carbon dioxide gas. 1.0 M HCL solution was added in 0.1 mL increments to the aqueous phase and the pH was monitored until it dropped to ~5.0. In addition, the $\%CO_2$ in the aqueous phase was monitored throughout using a CO_2 monitor (YSI 8500 CO_2 monitor - Yellow Springs, Ohio, USA).

For the dissolution experiments in bicarbonate buffer, different concentrations of bicarbonate buffer were prepared by adjusting quantities of 100% dry compressed air and 100% carbon dioxide in a 0.9%NaCl solution at appropriate ratios to make physiologically relevant concentrations of bicarbonate buffer. See Table 6 for the experimental parameters used for the dissolution tests. The $\%CO_2$(aq) in solution was determined using a CO_2 monitor (YSI 8500) and pH was monitored using a pH meter (Beckman Φ 40 - Brea, California, USA). The mixture of carbon dioxide gas and air was continuously pumped in throughout the dissolution runs to maintain bulk equilibrium. Solid sodium hydroxide and sodium hydroxide solution was added to adjust pH. The volume of the bicarbonate buffer dissolution medium for ibuprofen and indomethacin was 100 mL and for ketoprofen it was 200 mL. Differences in volume used for the experiments were made according to the solubility and predicted flux of each drug to achieve desirable experimental conditions (sink conditions and adequate sensitivity for UV analysis). All experiments were carried out at 100 rpm. However, dissolution tests for ibuprofen were also done at rotational speeds of 50, 250, and 500 rpm. Ibuprofen was also performed at bulk pH values 5.5, 6.0, and 7.0 (see Table 6 for buffer concentration at each pH).

The flux of the drug was predicted by applying the mathematical models outlined in this paper and the parameters that are given in Table 6 and 7 using MATLAB (MathWorks - Natick, Massachusetts, USA).

RESULTS

Bicarbonate Buffer Measured p*K*a

Figure 2 shows the measured pH as a function of the amount of 1.0 M HCl added during the titration and the experimental buffer capacity (dn/dpH) as a function of pH. This titration data suggest that the p*K*a of the bulk solution is ~6. A statistical analysis was performed by comparing the residual sum of squares and the result was a best fit bulk p*K*a of 6.04. This value was used for calculating the bulk bicarbonate buffer concentrations for all of the rotating disk dissolution experiments. Additionally, this was the p*K*a that was used in the BCE model for predicting drug flux in bicarbonate buffer. One factor to note is that bicarbonate concentration is continuously changing throughout the titration because the$\%CO_2$ increases as the pH decreases. However, it was observed in the bulk solution that CO_2 (aq) acts as a buffer component and therefore the total buffer concentration remains relatively constant. The measured value of 6.04 for the p*K*a of the overall reaction (Reaction 5) is consistent with experimentally determined values in the literature (Table 4).

Ibuprofen Results

Figure 3 shows the predicted impact of rotational speed (change in diffusion layer thickness) on the surface pH and the relative buffering ability of bicarbonate based on the different model approaches for ibuprofen. Assuming instantaneous

Table 7. Rotating Disk Dissolution Experimental Parameters Applied to the Weak Acid Drugs Examined

Drug			Ibuprofen		Indomethacin	Ketoprofen
Bulk pH	5.5	6.0	6.5	7.0	6.5	6.5
Percent CO_2	50	45	7–8, 14–16,[a] 21–22	5	7–8, 14–16, 21–22	7–8, 14–16, 24–26
Total buffer concentration $[CO_2(aq)]+[HCO_3^-]$ (mM)	15.5	20.7	6.5–7.5, 13–15*, 19.5–20.5	12.2	6.5–7.5, 13–15, 19.5–20.5	6.5–7.5, 13–15, 22–24
Bicarbonate concentration $[HCO_3^-]$ (mM)	3.5	9.9	5–5.5, 10–11,[a] 14.5–15.5	11	5–5.5, 10–11, 14.5–15.5	5–5.5, 10–11, 16.5–18.0
rpm	100	100	50, 100, 250, 500	100	100	100

[a]The concentration used for the ibuprofen experiments at 50, 250, and 500 rpm. For ibuprofen at pH 6.5 and 100 rpm, all buffer concentrations listed were used.

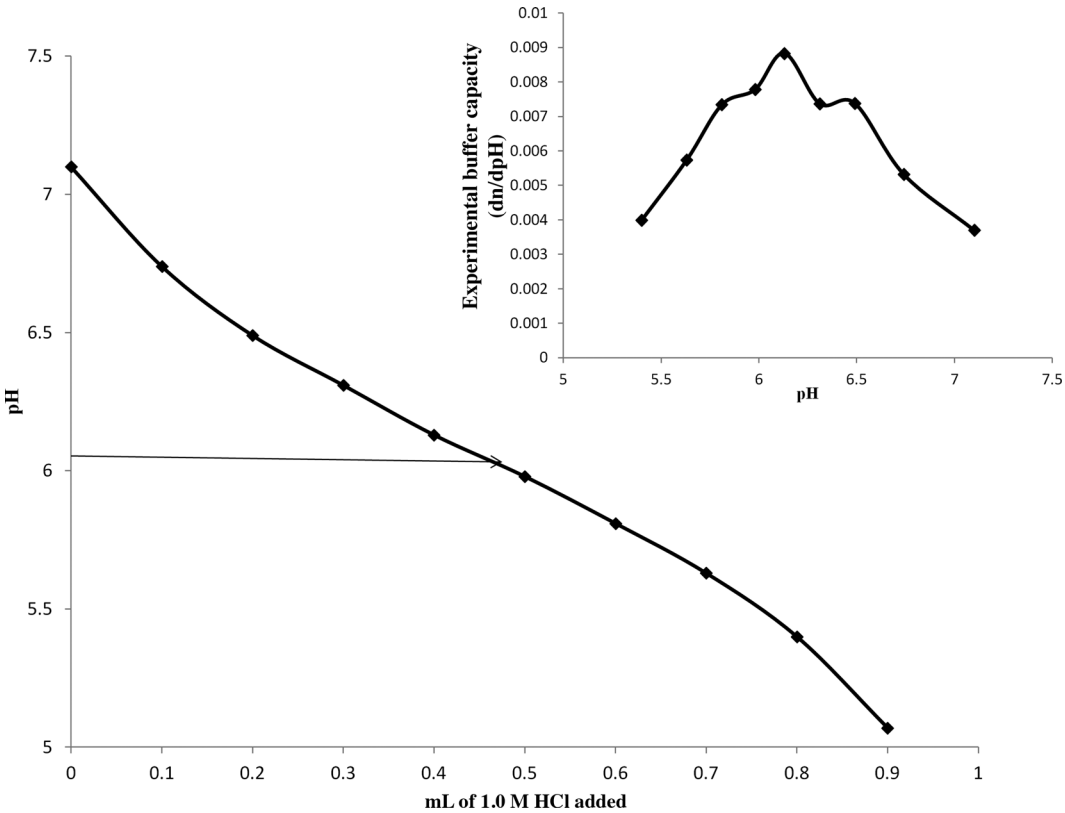

Figure 2. Titration curve for a closed bicarbonate buffer system at 37°C and isotonic ionic strength (0.154 M).

hydration/dehydration reactions (BCE model: p*K*a = 6.04) predicts bicarbonate to have the greatest buffer capacity and highest surface pH. When it is assumed that the hydration/dehydration reactions do not occur at all in the diffusion layer (CAI model: p*K*a 3.55), bicarbonate is predicted to have a low buffer capacity and low predicted surface pH. Assuming carbonic acid undergoes the irreversible dehydration reaction (IRR model), the predictions of buffer capacity and surface pH fall between the BCE and CAI models. Additionally, Figure 3 shows that the predicted surface pH decreases using the IRR model as the rotational speed increases. The thickness of the diffusion layer has no effect on surface pH for the BCE and CAI models because it is assumed that chemical equilibrium is achieved instantaneously in each case.

Figure 4 shows the experimental and predicted results for the flux of ibuprofen in bicarbonate buffer at different rotational speeds. As will be seen with all of the experimental data, the BCE model overestimates the effect bicarbonate buffer has on increasing the surface pH and the flux of ibuprofen. The CAI model underestimates the effect of bicarbonate buffer and the flux of ibuprofen. The flux predictions for the BCE and CAI models in Figure 4 are influenced only by the changing diffusion layer thickness as the rotational speed is changed because the surface pH is constant and independent of diffusion layer thickness (see Fig. 3). The predicted flux in the IRR model also depends on diffusion layer thickness but in a more complicated fashion. The surface pH is dependent on the residence time of the diffusing species, H_2CO_3, and this impacts the consumption

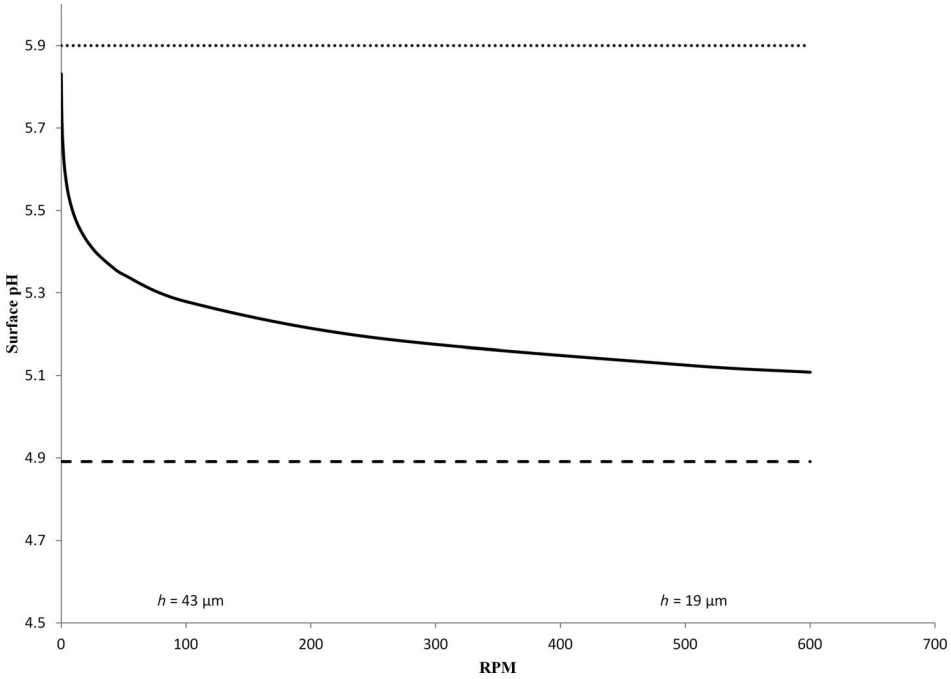

Figure 3. The predicted surface pH of ibuprofen in 10 mM bicarbonate buffer at pH 6.5 and different rotational speeds at 37°C. Key (.....) BCE model predictions; (▬▬▬) IRR model predictions; (▬ ▬ ▬) CAI model predictions.

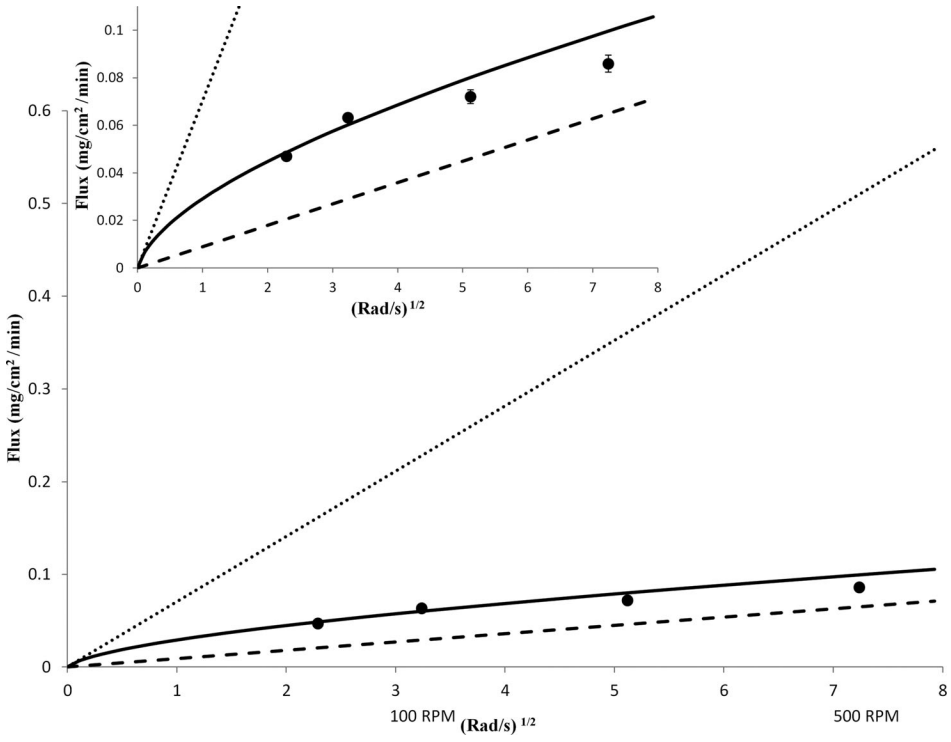

Figure 4. The experimental (50, 100, 250, and 500 rpm) and predicted flux of ibuprofen in 10 mM bicarbonate buffer ([HCO_3^-] only) at pH 6.5 and different rotational speeds at 37°C. Key (●) experimental flux; (..... .) BCE model flux predictions; (▬▬▬) IRR model flux predictions; (▬ ▬ ▬) CAI model flux predictions.

of H^+ through the irreversible dehydration reaction (see Fig. 3 and Appendix Eq. 34). The IRR model more accurately predicts the effect of a changing diffusion layer thickness as well as the diffusing species residence time in the diffusion layer on the ability of bicarbonate to buffer the pH at the surface of the dissolving drug.

Figure 5 shows the predicted and experimental flux of ibuprofen in bicarbonate buffer over a range of buffer

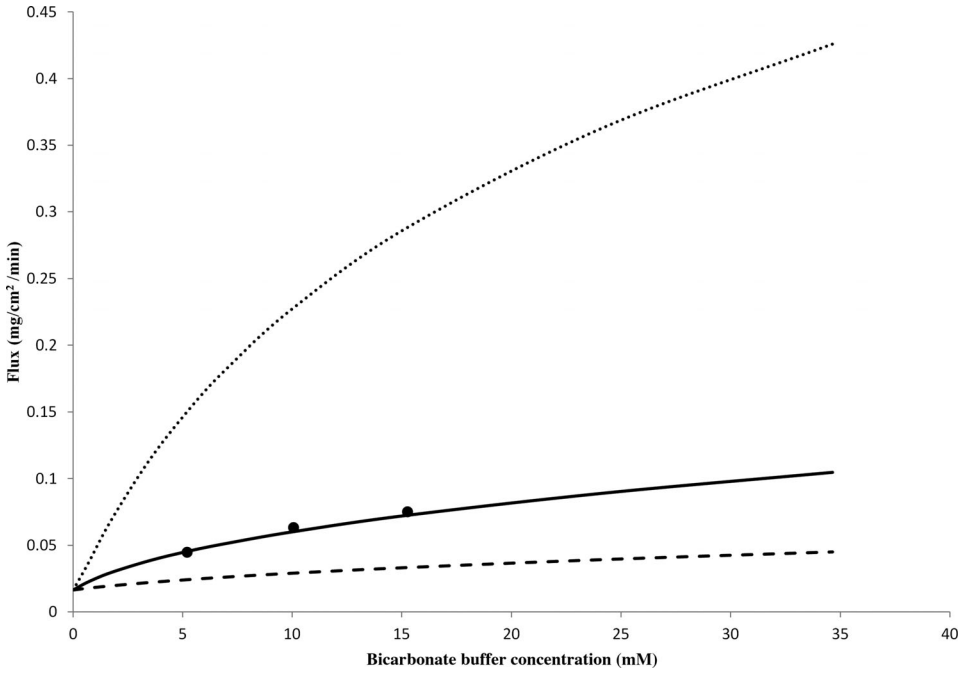

Figure 5. The experimental and predicted flux of ibuprofen in bicarbonate buffer ([HCO_3^-] only) at multiple concentrations (at pH 6.5 and 37°C). Key (●) experimental flux; (.....) BCE model flux predictions; (▬▬▬) IRR model flux predictions; (▬ ▬ ▬) CAI model flux predictions.

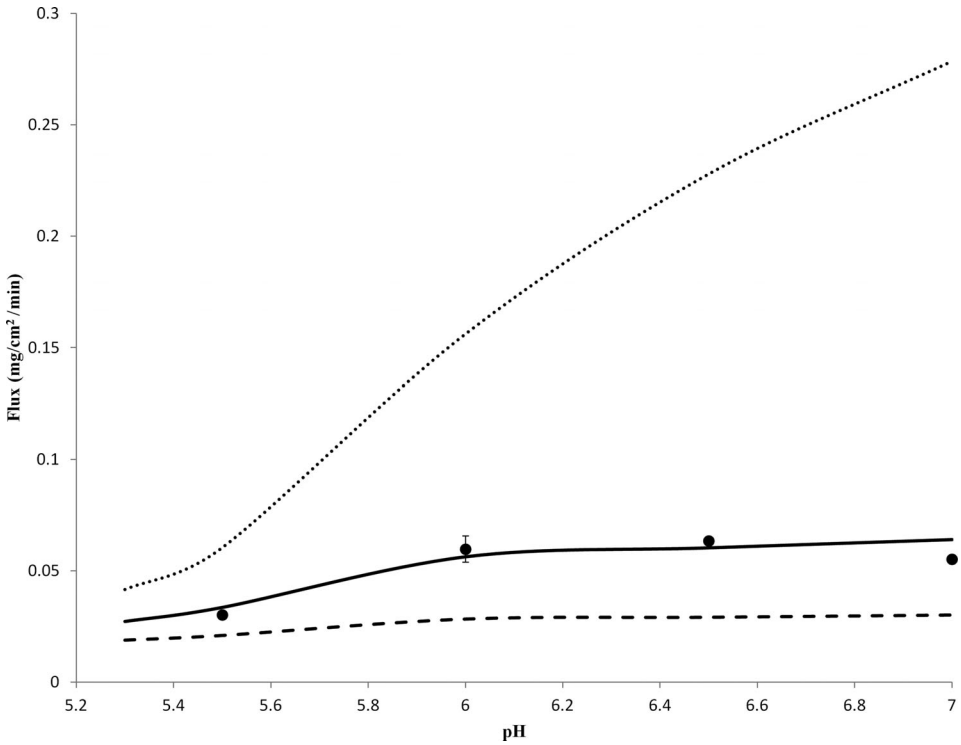

Figure 6. The experimental and predicted flux of ibuprofen in 10 mM bicarbonate buffer [HCO_3^-] only) at bulk pH values of 5.3(3.5 mM HCO_3^-), 6, 6.5, and 7 at 37°C. Key (●) experimental flux; (..... .) BCE model flux predictions; (▬▬▬) IRR model flux predictions; (▬ ▬ ▬) CAI model flux predictions.

concentrations at pH 6.5. There is a large difference in flux predictions when comparing the BCE versus CAI models. The experimental flux of ibuprofen in bicarbonate buffer falls between predictions assuming instantaneous hydration/dehydration reactions (BCE model) or no hydration/dehydration reactions (CAI model). When the hydration reaction is assumed to not occur and the dehydration reaction rate is incorporated into the mathematical analysis (IRR model), the predicted flux matches the experimental flux very well.

Figure 6 shows the effect bulk pH has on the flux of ibuprofen in 10–11 mM bicarbonate buffer at pH values of 6, 6.5, and 7 as well as 3.5 mM bicarbonate buffer at pH 5.5. The experimental

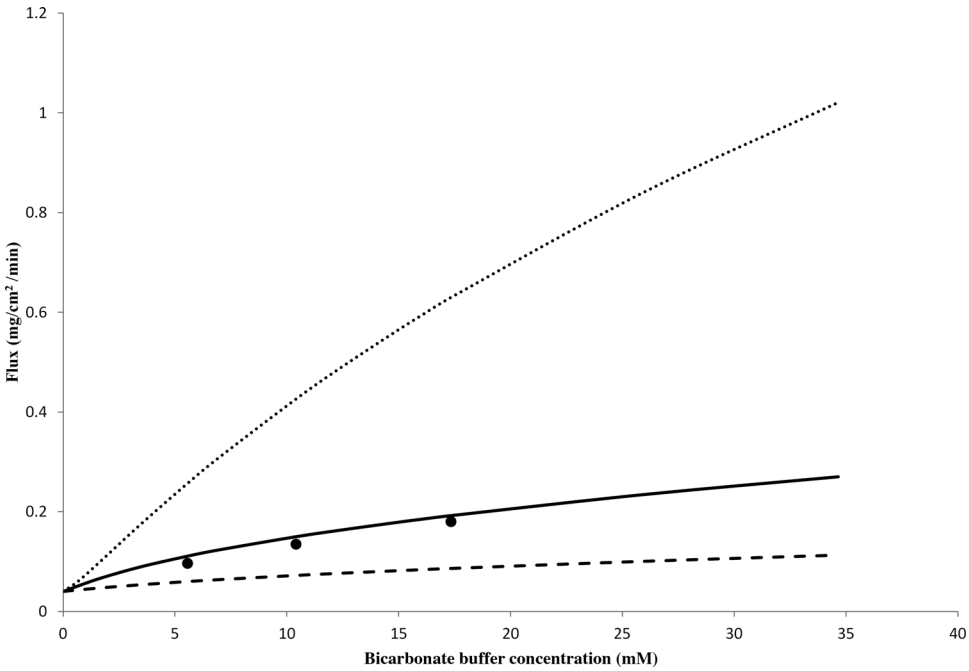

Figure 7. The experimental and predicted flux of ketoprofen in bicarbonate buffer ([HCO_3^-] only) at multiple concentrations (at pH 6.5 and 37°C). Key (●) experimental flux; (.....) BCE model flux predictions; (▬▬▬) IRR model flux predictions; (▬ ▬ ▬) CAI model flux predictions.

flux shows little variation as bulk solution pH is changed. The BCE model overestimates the effect that bulk pH and bicarbonate buffer have on increasing the pH at the surface of the dissolving drug and the flux of ibuprofen. The CAI model underestimates the effect that bulk pH and bicarbonate buffer have on increasing the pH at the surface of the dissolving drug and the flux of ibuprofen. The flux of ibuprofen in bicarbonate buffer over different bulk pH values is accurately predicted using the IRR model.

Ketoprofen Results

Figure 7 shows the experimental and predicted flux of ketoprofen in bicarbonate buffer over a range of buffer concentrations at pH 6.5. The predictions show that an increase in buffer concentration results in a significant increase in the flux. In comparison with ibuprofen, the solubility of ketoprofen is similar but it has a lower drug p*K*a. Therefore, ketoprofen acts as a similar self-buffer to ibuprofen but will be impacted by increasing buffer concentrations more under the experimental conditions. As was seen with ibuprofen, the experimental flux of ketoprofen in bicarbonate buffer is not predicted accurately by the BCE and CAI models and is only accurately predicted when the dehydration reaction rate is incorporated by applying the IRR model.

Indomethacin Results

Figure 8 shows the experimental and predicted flux of indomethacin in bicarbonate buffer over a range of buffer concentrations at pH 6.5. In comparison with ibuprofen and ketoprofen, the solubility of indomethacin is much lower. Therefore, indomethacin does not serve as an effective self-buffer, which leads to the surface pH approaching the bulk pH at low buffer concentrations. As was seen for with the other weak acid drugs, the experimental flux of indomethacin in bicarbonate buffer is not predicted accurately by the BCE or CAI models and is only accurately predicted by applying the IRR model.

To provide further confirmation for the accuracy of the IRR model, previous experimental work involving rotating disk dissolution in bicarbonate buffer was evaluated. A specific example is work by McNamara et al.[10] that also looked at the weak acid drug indomethacin using rotating disk dissolution. Their work focused on dissolution at different bicarbonate buffer concentrations (different bulk P_{CO_2}) at a bulk pH of 6.8. Figure 9 shows that the IRR model gives accurate predictions for the flux of indomethacin that was interpolated from the rotating disk experiments of McNamara et al. (Fig. 3 in their paper) using the parameters in Table 7 as well as the p*K*a for indomethacin that was reported in their paper (p*K*a = 4.17).

DISCUSSION

The results show that the ability of bicarbonate to buffer the surface pH of a dissolving drug is dependent on the hydration/dehydration reaction kinetics. The boundary layer IRR model predicts the pH at the surface of the dissolving drug and allows for accurate predictions of drug flux consistent with the mass transport analysis. The success of the boundary layer IRR model indicates that H_2CO_3 will form CO_2 and H_2O through an irreversible reaction in the diffusion layer while undergoing its instantaneous, reversible ionization reaction to form bicarbonate. The IRR model, in effect, means that bicarbonate buffer behaves differently at the solid surface and in the boundary layer of a dissolving drug than it does in the bulk dissolution medium where the hydration/dehydration reaction is at equilibrium. In effect, bicarbonate has a "dynamic buffer capacity" represented by the IRR model at the dissolving surface and boundary layer where the hydration reaction can be assumed to not occur while it has the standard buffer capacity expected of bicarbonate buffer in the bulk.

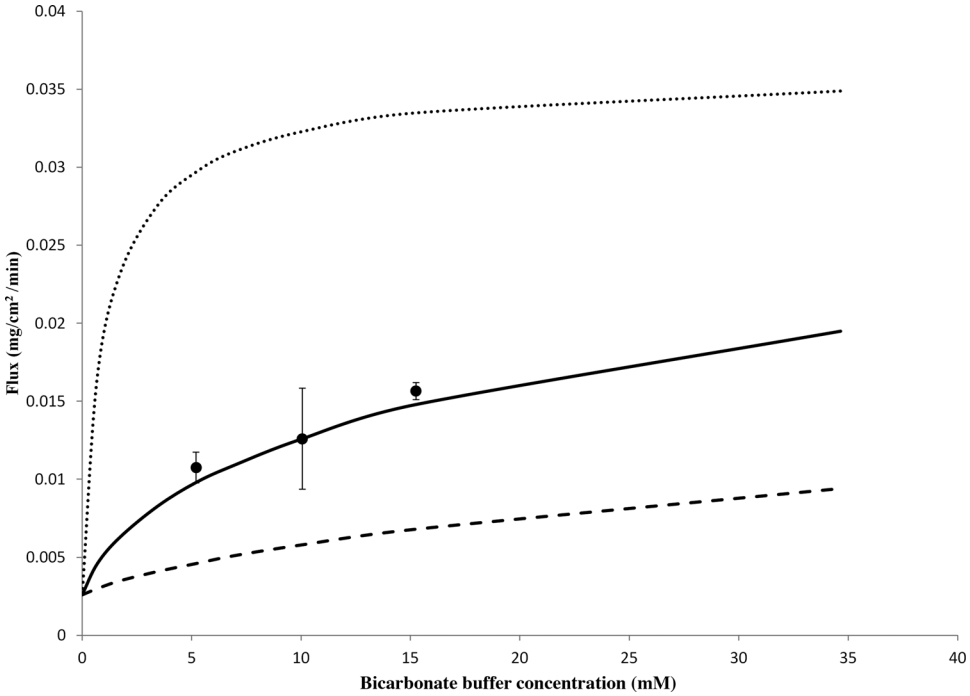

Figure 8. The experimental and predicted flux of indomethacin in bicarbonate buffer ([HCO_3^-] only) at multiple concentrations (at pH 6.5 and 37°C). Key (●) experimental flux; (.....) BCE model flux predictions; (▬▬▬) IRR model flux predictions; (▬ ▬ ▬) CAI model flux predictions.

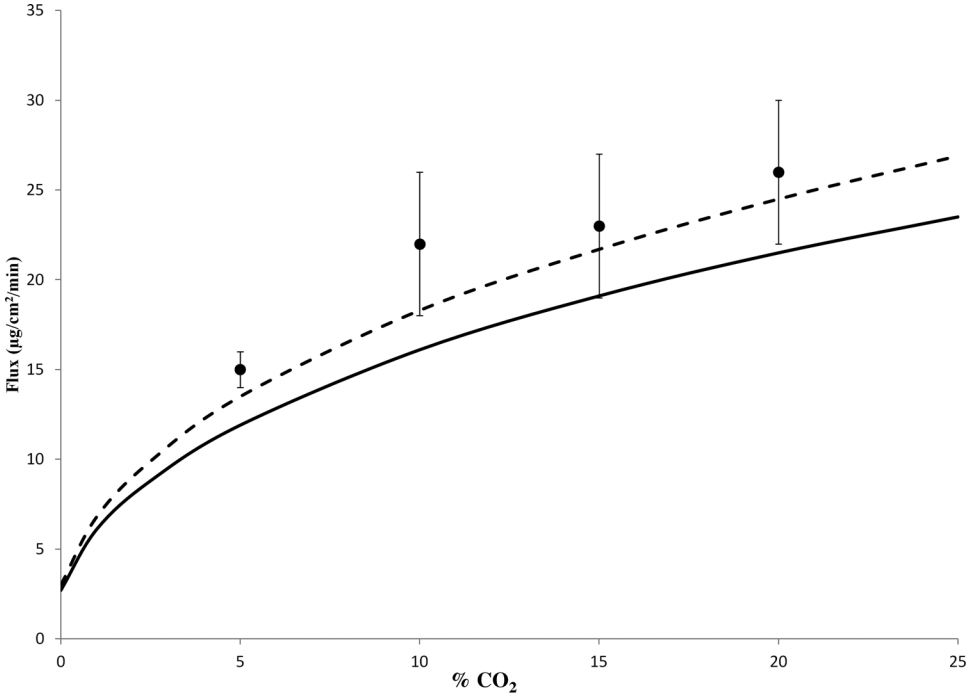

Figure 9. The experimental (data interpolated from Fig. 3 of McNamara et al.[10]) and predicted flux of indomethacin in bicarbonate buffer at multiple concentrations (at pH 6.8 and 37°C). Key (●) experimental flux; (▬ ▬ ▬) IRR model flux predictions based on indomethacin p*K*a = 4.17; (▬▬▬) IRR model flux predictions based on indomethacin p*K*a = 4.27.

Based on drug solubility and drug p*K*a, each drug studied has a different self-buffering effect at its dissolving surface. The results show that the IRR model accurately predicts surface pH and drug flux even when large differences in drug properties exist. For example, indomethacin has an intrinsic solubility ~100 times lower than ibuprofen and ketoprofen but this does not impact the accuracy of the predictions. Additionally, the ibuprofen and indomethacin data from this paper and from McNamara et al. show the robustness of the IRR model to changes in experimental conditions and the accuracy of the IRR

model to be replicated in different laboratories. The IRR model can accurately account for surface pH changes when the bulk pH and diffusion layer thickness is altered. When the diffusion layer thickness decreases, less time is available for the protons that have formed H_2CO_3 to undergo the dehydration reaction and form CO_2 and H_2O. This changes the ability of bicarbonate to function as a buffer and it becomes similar to a situation where only the ionization reaction occurs. Therefore, changing the rotational speed of the disk will change the surface pH and this can be well accounted for by the IRR model. The impact on surface pH that results from the changing diffusion layer thickness in the IRR model is one of the many factors taken into account in the cubic equation (Appendix Eq. (34)) that calculates the pH at the surface of the dissolving drug. The IRR and the CAI models have different mass transfer coefficients for the flux of carbonic acid. The mass transfer coefficient of carbonic acid for the IRR model is $\sqrt{k_d D_{H_2CO_3}}$ and the mass transfer coefficient for the CAI model is $\frac{D_{H_2CO_3}}{h}$. When the ratio of the mass transfer coefficients equals one ($h = 5.4\ \mu m$) then the pH at the surface becomes equal to the CAI model because the irreversible reaction is no longer consuming protons that will allow for an increase in the buffer capacity beyond the CAI model. Conversely, Figures 3 and 4 show that as the diffusion layer thickness becomes larger, the proton consumption caused by the irreversible chemical reaction increases, which allows for the IRR model to provide a similar buffer effect that is seen in the BCE model, However, this effect would only occur at unrealistically large diffusion layer thickness values.

Although bicarbonate is the buffer present in the GI tract, using it as a buffer in dissolution testing is challenging because of long preparation times and hydrodynamic concerns (i.e., presence of air and CO_2 gas bubbles in the apparatus) that make it less than ideal. However, the accuracy of the IRR model in predicting drug flux in bicarbonate buffer using known physicochemical parameters allows for the possibility of predicting a more physiologically relevant buffer based on the physicochemical properties of the drug. Aunins et al.[3] demonstrated that the dissolution of weak acid drugs can be accurately predicted in standard buffers (i.e., phosphate) using the standard film model. The accuracy of these models creates the basis for the development of an *in vitro* dissolution buffer system with more standard buffers that would be more predictive of the *in vivo* buffer conditions. However, the work carried out in this paper and by Aunins et al.[3] applies only to rotating disk dissolution with fixed experimental conditions in the bulk solution. A dissolving ionizable dosage form could have an effect on the bulk pH or introduce additional ionic or buffering species that could impact experimental and predicted dissolution rates. Additionally, the dynamic nature of the *in vivo* environment with dynamic intestinal secretion of bicarbonate, the absorption of water, and transit through the intestine continues to make prediction of *in vivo* dissolution complex.

CONCLUSIONS

Applying the boundary layer model with the assumption of instantaneous BCE (BCE model) does not accurately predict the buffer capacity of bicarbonate in the diffusion layer of a dissolving drug. Assuming that the hydration and dehydration reactions happen instantaneously overestimates the ability of bicarbonate to buffer the pH at the surface of the dissolving drug. On the other hand, assuming that both the dehydration and hydration reactions are too slow to occur in the diffusion layer (CAI model) underestimates the impact of bicarbonate buffer in the diffusion layer and at the surface of the tablet.

The predicted and experimental flux in bicarbonate buffer indicates the importance of the reaction kinetics in the bicarbonate buffer system. The effect of the slow hydration reaction in the diffusion layer has a significant impact on the buffer capacity of bicarbonate at the surface of a dissolving drug and drug dissolution. The assumption that CO_2 does not react with H_2O in the diffusional boundary layer, and thus assuming that H_2CO_3 undergoes an irreversible chemical reaction forming CO_2 and H_2O in addition to its ionization reaction (pKa = 3.55), accurately predicts the effect that bicarbonate buffer has on the pH in the diffusion layer. The IRR model is intermediate between the BCE and CAI models and most accurately describes the experimental results. In effect, bicarbonate has: (a) a "dynamic buffer capacity" represented by the IRR model at the dissolving surface where the hydration reaction can be assumed to not occur and, (b) the standard buffer capacity expected of bicarbonate buffer in the bulk where the hydration reaction can be assumed to occur sufficiently quickly to appear to be instantaneous (i.e., is at equilibrium). The irreversible reaction in the diffusion layer where H_2CO_3 forms CO_2 and H_2O allows protons to be consumed and assists in buffering the pH at the surface of the tablet. The protons consumed by the irreversible reaction is a function of the time H_2CO_3 spends in the diffusion boundary layer and is therefore dependent on the thickness of the diffusion layer. Unlike the film models, assuming instantaneous chemical equilibrium (BCE and CAI), the pH at the surface in the IRR model is a function of diffusion layer thickness.

The IRR model has been shown to accurately predict the rotating disk dissolution rate of the weak acid drugs studied. More experimental work is needed to assess its applicability to weak bases and amphoteric drugs. However, for ionizable drugs, the pH at the surface is a key component in determining the rate at which the drug will dissolve, and the IRR model is accurate at predicting surface pH under various experimental conditions examined in this paper. Therefore, the IRR model may be used to identify buffers that more closely resemble the bicarbonate buffer of the luminal fluid and provide an approach for the development of more relevant *in vivo* dissolution media.

ACKNOWLEDGMENTS

Financial support provided by USP Fellowship (2010–2012), the Chingju Wang Sheu Graduate Student Fellowship (2009–2011) AstraZeneca Grant, and FDA Contract HHSF223201310144C is gratefully acknowledged.

APPENDIX

Irreversible reaction (IRR) model for the dissolution of weak acid drugs (HA = unionized form of the weak acid drug; A^- = ionized form of the weak acid drug) in bicarbonate buffer. Below are the equilibrium reactions before the irreversible dehydration reaction assumption is introduced:

$$H^+ + OH^- \overset{K_w}{\rightleftarrows} H_2O$$

$$HA \overset{K_a^A}{\rightleftarrows} H^+ + A^-$$

$$HA + OH^- \overset{K_1^*}{\rightleftarrows} H_2O + A^-$$

$$HA + HCO_3^- \overset{K_2}{\rightleftarrows} H_2CO_3 + A^-$$

$$CO_2 + H_2O \overset{K_C}{\rightleftarrows} H_2CO_3$$

$$H_2CO_3 \overset{K_{al}}{\rightleftarrows} HCO_3^- + H^+$$

$CO_2 + OH^- \rightleftarrows^{k_{a2}} HCO_3^-$ is not considered because research has shown that this reaction would not play a role at the pH the experiments were performed at.[50]

Chemical equilibrium constant equations:

$$K_w = [H^+][OH^-] \tag{A1}$$

$$K_a^A = \frac{[A^-][H^+]}{[HA]} \tag{A2}$$

$$K_1 = \frac{[A^-]}{[HA][OH^-]} = \frac{K_a^A}{K_W} \tag{A3}$$

$$K_2 = \frac{[A^-][H_2CO_3]}{[HA][HCO_3^-]} = \frac{K_a^A}{K_{a1}} \tag{A4}$$

$$K_c = \frac{[H_2CO_3]}{[CO_2]} = \frac{k_h}{k_d} \tag{A5}$$

$$K_{a1} = \frac{[HCO_3^-][H^+]}{[H_2CO_3]} = \frac{k_{a1f}}{k_{a1r}} \tag{A6}$$

Differential equations defining the flux of the different species:

$$\frac{\delta[HA]}{\delta t} = D_{HA}\frac{\delta^2[HA]}{\delta X^2} + \emptyset_1 = 0 \tag{A7}$$

$$\frac{\delta[A^-]}{\delta t} = D_A\frac{\delta^2[A^-]}{\delta X^2} + \emptyset_2 = 0 \tag{A8}$$

$$\frac{\delta[H^+]}{\delta t} = D_H\frac{\delta^2[H^+]}{\delta X^2} + \emptyset_3 = 0 \tag{A9}$$

$$\frac{\delta[OH^-]}{\delta t} = D_{OH}\frac{\delta^2[OH^-]}{\delta X^2} + \emptyset_4 = 0 \tag{A10}$$

$$\frac{\delta[HCO_3^-]}{\delta t} = D_{HCO_3}\frac{\delta^2[HCO_3^-]}{\delta X^2} + \emptyset_5 = 0 \tag{A11}$$

$$\frac{\delta[H_2CO_3]}{\delta t} = D_{H_2CO_3}\frac{\delta^2[H_2CO_3]}{\delta X^2} + \emptyset_6 = 0 \tag{A12}$$

$$\frac{\delta[CO_2]}{\delta t} = D_{CO_2}\frac{\delta^2[CO_2]}{\delta X^2} + \emptyset_7 = 0 \tag{A13}$$

Defining Ø 1–7 for the differential equations:

$$\emptyset_1 = -k_{af}^A[HA] + k_{ar}^A[H^+][A^-] - k_{1f}[HA][OH^-] + k_{1r}[A^-] - k_{2f}[HA][HCO_3^-] + k_{2r}]\,H_2CO_3][A^-]$$

$$\emptyset_2 = k_{af}^A[HA] - k_{ar}^A[H^+][A^-] + k_{1f}[HA][OH^-] - k_{1r}[A^-] + K_{2f}[HA][HCO_3^-] - k_{2r}[H_2CO_3][A^-]$$

$$\emptyset_3 = k_{af}^A[HA] - k_{ar}^A[H^+][A^-] + k_{a1f}[H_2CO_3] - k_{a1r}[H^+][HCO_3^-]$$

$$\emptyset_4 = -k_{1f}[HA][OH^-] + k_{1r}[A^-]$$

$$\emptyset_5 = -K_{2f}[HA][HCO_3^-] + K_{2r}[H_2CO_3][A^-] + k_{a1f}[H_2CO_3] - k_{a1r}[H^+][HCO_3^-]$$

$$\emptyset_6 = k_{2f}[HA][HCO_3^-] - k_{2r}[H_2CO_3][A^-] + k_h[CO_2] - k_d[H_2CO_3] - k_{a1f}[H_2CO_3] + k_{a1r}[H^+][HCO_3^-]$$

$$\emptyset_7 = -k_h[CO_2] + k_d[H_2CO_3]$$

Setting up relations for Ø and the diffusion terms based on assumptions from Mooney et al.[1]:

The first relation is that the amount of components reacting as acids must equal the amount of components acting as bases.

$$\emptyset_4 + \emptyset_5 = \emptyset_1 + \emptyset_3 \tag{A14}$$

Equation (A14) based on the definitions for phi above:

$$\begin{aligned}&(-k_{1f}[HA][OH^-] + k_{1r}[A^-]) + (-k_{2f}[HA][HCO_3^-]\\&+ k_{2r}[H_2CO_3][A^-] + k_{a1f}[H_2CO_3] - k_{a1r}[H^+][HCO_3^-])\\&= (-k_{af}^A[HA] + K_{ar}^A[H^+][A^-] - k_{1f}[HA][OH^-] + k_{1r}[A^-]\\&-k_{2f}[HA][HCO_3^-] + k_{2r}[H_2CO_3][A^-]) + (k_{af}^A[HA]\\&-k_{ar}^A[H^+][A^-] + k_{a1f}[H_2CO_3] - k_{a1r}[H^+][HCO_3^-])\end{aligned} \tag{A15}$$

The like terms cancel on each side of the above equation which leads to Eq. (A15) becoming: $0 = 0$

The second assumption is that the acid drug in solution is neither created nor destroyed.

$$\emptyset_1 + \emptyset_2 = 0 \tag{A16}$$

Equation (A16) based on the definitions for phi above:

$$\begin{aligned} 0 = (&-k_{\mathrm{af}}^{\mathrm{A}}[\mathrm{HA}] + k_{\mathrm{ar}}^{\mathrm{A}}[\mathrm{H}^+][\mathrm{A}^-] - k_{1\mathrm{f}}[\mathrm{HA}][\mathrm{OH}^-] \\ &+ k_{1\mathrm{r}}[\mathrm{A}^-] - k_{2\mathrm{f}}[\mathrm{HA}][\mathrm{HCO}_3^-] + k_{2\mathrm{r}}[\mathrm{H_2CO_3}][\mathrm{A}^-]) \\ &+ (k_{\mathrm{af}}^{\mathrm{A}}[\mathrm{HA}] - k_{\mathrm{ar}}^{\mathrm{A}}[\mathrm{H}^+][\mathrm{A}^-] + k_{1\mathrm{f}}[\mathrm{HA}][\mathrm{OH}^-] \\ &-k_{1\mathrm{r}}[\mathrm{A}^-] + k_{2\mathrm{f}}[\mathrm{HA}][\mathrm{HCO}_3^-] - k_{2\mathrm{r}}[\mathrm{H_2CO_3}][\mathrm{A}^-]) \end{aligned}$$

Equation (A16) allows for the relation made in Eq. (A17) based on the assumption of steady state.

$$D_{\mathrm{HA}}\frac{\delta^2\left[\mathrm{HA}\right]}{\delta X^2} + D_{\mathrm{A}}\frac{\delta^2\left[\mathrm{A}^-\right]}{\delta X^2} = 0 \tag{A17}$$

The third assumption is that since k_{h} is so small ($\sim$0.1–0.16 s^{-1}) it is going to be assumed that it is not playing a role in formation of any H_2CO_3 in the diffusion layer. Therefore, H_2CO_3 is undergoing an irreversible chemical reaction to form CO_2 and H_2O in addition to the reversible ionization reaction that forms H^+ and HCO_3^-. The change in carbon dioxide concentration has no effect on the other buffer components leading to the IRR model.

$$\mathrm{CO_2\,(aq) + H_2O} \overset{k_{\mathrm{d}}}{\leftarrow} \mathrm{H_2CO_3} \overset{K_1}{\underset{\rightarrow}{\leftarrow}} \mathrm{H^+ + HCO_3^-}$$

Therefore, it is assumed that the only two buffer components are H_2CO_3 and HCO_3^-. The change in bicarbonate is based only upon the change in carbonic acid. This assumption leads to Eq. (A18):

$$\begin{aligned} &D_{\mathrm{HCO_3}}\frac{\delta^2[\mathrm{HCO_3^-}]}{\delta X^2} - k_{2\mathrm{f}}[\mathrm{HA}][\mathrm{HCO_3^-}] + k_{2\mathrm{r}}[\mathrm{H_2CO_3}][\mathrm{A}^-] \\ &\quad + k_{\mathrm{a1f}}[\mathrm{H_2CO_3}] - k_{\mathrm{a1r}}[\mathrm{H}^+][\mathrm{HCO_3^-}] \\ &= -\left(D_{\mathrm{H_2CO_3}}\frac{\delta^2[\mathrm{H_2CO_3}]}{\delta X^2} + k_{2\mathrm{f}}[\mathrm{HA}][\mathrm{HCO_3^-}] - k_{2\mathrm{r}}[\mathrm{H_2CO_3}][\mathrm{A}^-]\right. \\ &\quad \left. - k_{\mathrm{a1f}}[\mathrm{H_2CO_3}] + k_{\mathrm{a1r}}[\mathrm{H}^+][\mathrm{HCO_3^-}] - k[\mathrm{H_2CO_3}]\right) \end{aligned} \tag{A18}$$

All of the like terms cancel and Eq. (A18) simplifies to Eq. (A19).

$$\begin{aligned} &D_{\mathrm{HCO_3}}\frac{\delta^2\left[\mathrm{HCO_3^-}\right]}{\delta X^2} \\ &\quad = -\left(D_{\mathrm{H_2CO_3}}\frac{\delta^2\left[\mathrm{H_2CO_3}\right]}{\delta X^2} - k_{\mathrm{d}}\left[\mathrm{H_2CO_3}\right]\right) \end{aligned} \tag{A19}$$

At this point, all of the second order differential equations can be solved. For all of the terms that are diffusion controlled, the boundary conditions and general solution are shown below.

$$D_{\mathrm{C}}\frac{\delta^2\,[C]}{\delta X^2} = 0 \tag{A20}$$

Boundary conditions:

$$\text{a t}x = h; C = C_{\mathrm{h}}$$

$$\text{a t}x = 0; C = C_0$$

The general solution to the second order differential is shown below.

$$c = \frac{(C_{\mathrm{h}} - C_{\mathrm{o}})\,x}{h} + C_0 \tag{A21}$$

H_2CO_3 is not only diffusion controlled because it also undergoes an irreversible chemical reaction. The boundary conditions are the same for the species but its general solution is different.

$$D_{\mathrm{H_2CO_3}}\frac{\delta^2\left[\mathrm{H_2CO_3}\right]}{\delta X^2} - k_{\mathrm{d}}\left[\mathrm{H_2CO_3}\right] = 0 \tag{A22}$$

$$D_{\mathrm{H_2CO_3}}\frac{\delta^2\left[\mathrm{H_2CO_3}\right]}{\delta X^2} = k_{\mathrm{d}}\left[\mathrm{H_2CO_3}\right]$$

Boundary conditions:

$$\text{a t}x = h; C = \left[\mathrm{H_2CO_3}\right]_{\mathrm{h}}$$

$$\text{a t}x = 0; C = \left[\mathrm{H_2CO_3}\right]_0$$

The general solution to the second order differential for carbonic acid is shown below.

$$\begin{aligned} &\frac{\left(-[\mathrm{H_2CO_3}]_0 e^{-\frac{\sqrt{k_{\mathrm{d}}}}{\sqrt{D_{\mathrm{H_2CO_3}}}}h} + [\mathrm{H_2CO_3}]_{\mathrm{h}}\right) e^{\frac{\sqrt{k_{\mathrm{d}}}}{\sqrt{D_{\mathrm{H_2CO_3}}}}x}}{e^{\frac{\sqrt{k_{\mathrm{d}}}}{\sqrt{D_{\mathrm{H_2CO_3}}}}h} - e^{-\frac{\sqrt{k_{\mathrm{d}}}}{\sqrt{D_{\mathrm{H_2CO_3}}}}h}} \\ &- \frac{\left([\mathrm{H_2CO_3}]_{\mathrm{h}} - [\mathrm{H_2CO_3}]_0 e^{\frac{\sqrt{k_{\mathrm{d}}}}{\sqrt{D_{\mathrm{H_2CO_3}}}}h}\right) e^{-\frac{\sqrt{k_{\mathrm{d}}}}{\sqrt{D_{\mathrm{H_2CO_3}}}}x}}{e^{\frac{\sqrt{k_{\mathrm{d}}}}{\sqrt{D_{\mathrm{H_2CO_3}}}}h} - e^{-\frac{\sqrt{k_{\mathrm{d}}}}{\sqrt{D_{\mathrm{H_2CO_3}}}}h}} \end{aligned} \tag{A23a}$$

The diffusion coefficient of carbonic acid is a constant ($D_{\mathrm{H_2CO_3}} = 14.6 \times 10^{-6}$ $\mathrm{cm^2/s}$) and so is the dehydration rate constant ($k_{\mathrm{d}} = 50\,\mathrm{s}^{-1}$). The diffusion layer thickness changes based on the Levich equation but it is on the order of 0.001–0.005. Therefore, $e^{-\frac{\sqrt{k_{\mathrm{d}}}}{\sqrt{D_{\mathrm{H_2CO_3}}}}h}$ is so small ($\sim 4 \times 10^{-5}$) in comparison with $e^{\frac{\sqrt{k_{\mathrm{d}}}}{\sqrt{D_{\mathrm{H_2CO_3}}}}h}$ ($\sim 2.5 \times 10^4$) that it can be assumed

that $e^{-\frac{\sqrt{k_d}}{\sqrt{D_{H_2CO_3}}}h}$ and $-\left[H_2CO_3\right]_0 e^{-\frac{\sqrt{k_d}}{\sqrt{D_{H_2CO_3}}}h}$ ($\sim 10^{-7}$–10^{-9}) and $\left[H_2CO_3\right]_h e^{-\frac{\sqrt{k_d}}{\sqrt{D_{H_2CO_3}}}h}$ ($\sim 10^{-9}$–10^{-10}) is equal to zero and equation (A23a) becomes Eq. (A23b).

$$\frac{[H_2CO_3]_h e^{\frac{\sqrt{k_d}}{\sqrt{D_{H_2CO_3}}}x}}{e^{\frac{\sqrt{k_d}}{\sqrt{D_{H_2CO_3}}}h}} - \frac{\left([H_2CO_3]_0 e^{\frac{\sqrt{k_d}}{\sqrt{D_{H_2CO_3}}}h}\right) e^{-\frac{\sqrt{k_d}}{\sqrt{D_{H_2CO_3}}}x}}{e^{\frac{\sqrt{k_d}}{\sqrt{D_{H_2CO_3}}}h}} \tag{A23b}$$

In order to apply the rest of the assumptions to the film model, the derivative to all of the general solutions must be obtained in order to define all of the species in terms of flux.

Taking the derivative of all of the diffusion controlled species gives the equation below:

$$\frac{\partial [C]}{\partial X} = \frac{(C_h - C_o)}{h} \tag{A24}$$

Equation (A24) must be multiplied by the diffusion coefficient to give the flux of the species.

$$D\frac{\partial [C]}{\partial X} = D\frac{(C_h - C_o)}{h} \tag{A25}$$

Taking the derivative of the general solution for H_2CO_3 (Eq. (A23b) gives Eq. (A26).

$$\frac{[H_2CO_3]_h \sqrt{k_d} e^{\frac{\sqrt{k_d}}{\sqrt{D_{H_2CO_3}}}x}}{\sqrt{D_{H_2CO_3}} e^{\frac{\sqrt{k_d}}{\sqrt{D_{H_2CO_3}}}h}} - \frac{[H_2CO_3]_0 \sqrt{k_d} e^{-\frac{\sqrt{k_d}}{\sqrt{D_{H_2CO_3}}}x}}{\sqrt{D_{H_2CO_3}}} \tag{A26}$$

In order to solve for the flux from $x = h$ to $x = 0$, the h and x must be inserted into Eq. (A26).

At $x = 0$

$$\frac{\left[H_2CO_3\right]_h \sqrt{k_d} e^{\frac{\sqrt{k_d}}{\sqrt{D_{H_2CO_3}}}0}}{\sqrt{D_{H_2CO_3}} e^{\frac{\sqrt{k_d}}{\sqrt{D_{H_2CO_3}}}h}} - \frac{\left[H_2CO_3\right]_0 \sqrt{k_d} e^{-\frac{\sqrt{k_d}}{\sqrt{D_{H_2CO_3}}}0}}{\sqrt{D_{H_2CO_3}}} \tag{A27}$$

$e^{\frac{\sqrt{k_d}}{\sqrt{D_{H_2CO_3}}}0}$ is equal to 1 which simplifies the above equation:

$$\frac{\left[H_2CO_3\right]_h \sqrt{k_d}}{\sqrt{D_{H_2CO_3}} e^{\frac{\sqrt{k_d}}{\sqrt{D_{H_2CO_3}}}h}} - \frac{\left[H_2CO_3\right]_0 \sqrt{k_d}}{\sqrt{D_{H_2CO_3}}}$$

$\sqrt{D_{H_2CO_3}}\, e^{\frac{\sqrt{k_d}}{\sqrt{D_{H_2CO_3}}}h}$ ($\sim$0.4) $\gg \left[H_2CO_3\right]_h \sqrt{k_d}$ ($\sim 10^{-4}$–10^{-5}) that $\frac{\left[H_2CO_3\right]_h \sqrt{k_d}}{\sqrt{D_{H_2CO_3}}\, e^{\frac{\sqrt{k_d}}{\sqrt{D_{H_2CO_3}}}h}}$ is considered to be zero which leaves:

$$-\frac{\left[H_2CO_3\right]_0 \sqrt{k_d}}{\sqrt{D_{H_2CO_3}}}$$

At $x = h$

$$\frac{\left[H_2CO_3\right]_h \sqrt{k_d} e^{\frac{\sqrt{k_d}}{\sqrt{D_{H_2CO_3}}}h}}{\sqrt{D_{H_2CO_3}} e^{\frac{\sqrt{k_d}}{\sqrt{D_{H_2CO_3}}}h}} - \frac{\left[H_2CO_3\right]_0 \sqrt{k_d} e^{-\frac{\sqrt{k_d}}{\sqrt{D_{H_2CO_3}}}h}}{\sqrt{D_{H_2CO_3}}}$$

$e^{-\frac{\sqrt{k_d}}{\sqrt{D_{H_2CO_3}}}h}$ is so small ($\sim 4 \times 10^{-5}$) that it can be assumed that it and $-\left[H_2CO_3\right]_0 \sqrt{k_d} e^{-\frac{\sqrt{k_d}}{\sqrt{D_{H_2CO_3}}}h} = 0$

$$\frac{\left[H_2CO_3\right]_h \sqrt{k_d}}{\sqrt{D_{H_2CO_3}}}$$

Therefore $\frac{\partial[H_2CO_3]}{\partial x}$ from $x = h$ (bulk solution) to the surface of the tablet ($x = 0$) is

$$\frac{\partial\left[H_2CO_3\right]}{\partial x} = \frac{\sqrt{k_d}}{\sqrt{D_{H_2CO_3}}}\left(\left[H_2CO_3\right]_h - \left[H_2CO_3\right]_0\right) \tag{A28}$$

If you multiply each side by the diffusion coefficient of carbonic acid, then that will give the flux of carbonic acid.

$$D_{H_2CO_3}\frac{\partial\left[H_2CO_3\right]}{\partial x} = \left(\left[H_2CO_3\right]_h - \left[H_2CO_3\right]_0\right)\sqrt{D_{H_2CO_3}k_d} \tag{A29}$$

It is assumed that electric neutrality is maintained at every point in the diffusion layer so the positively charged species flux must be equal to the negatively charged species flux.

$$\sum z_i J_i = 0 \tag{A30}$$

$$D_H\frac{\left(\left[H^+\right]_h - \left[H^+\right]_0\right)}{h} = D_{OH}\frac{\left(\left[OH^-\right]_h - \left[OH^-\right]_0\right)}{h} + D_A\frac{\left(\left[A^-\right]_h - \left[A^-\right]_0\right)}{h} + D_{HCO_3}\frac{\left(\left[HCO_3^-\right]_h - \left[HCO_3^-\right]_0\right)}{h} \tag{A31}$$

Another assumption is that since no boundary or internal sources of buffer exist, then the total buffer flux must be equal to 0.

$$D_{HCO_3}\frac{\left(\left[HCO_3^-\right]_h - \left[HCO_3^-\right]_0\right)}{h} + \left(\left[H_2CO_3\right]_h - \left[H_2CO_3\right]_0\right)\sqrt{D_{H_2CO_3}k_d} = 0 \tag{A32}$$

$$D_{HCO_3}\frac{\left(\left[HCO_3^-\right]_h-\left[HCO_3^-\right]_0\right)}{h}=-\left(\left[H_2CO_3\right]_h-\left[H_2CO_3\right]_0\right)\sqrt{D_{H_2CO_3}k_d} \quad \text{(A33)}$$

Equation (33) can be used to find the concentration of bicarbonate at the surface of the tablet. First it must be put in terms of known values and H^+ at the surface of the tablet as shown below.

$$D_{HCO_3}\left(\left[HCO_3^-\right]_h-\left[HCO_3^-\right]_0\right)=-\left(\left[H_2CO_3\right]_h-\left[H_2CO_3\right]_0\right)h\sqrt{D_{H_2CO_3}k_d}$$

$$-D_{HCO_3}\left[HCO_3^-\right]_0-\left[H_2CO_3\right]_0\left(h\sqrt{D_{H_2CO_3}k_d}\right)=-\left[H_2CO_3\right]_h\left(h\sqrt{D_{H_2CO_3}k_d}\right)-D_{HCO_3}\left[HCO_3^-\right]_h$$

$$\left[H_2CO_3\right]_0=\frac{\left[HCO_3^-\right]_0\left[H^+\right]_0}{K_{a1}}$$

$$D_{HCO_3}\left[HCO_3^-\right]_0+\frac{\left[HCO_3^-\right]_0\left[H^+\right]_0}{K_{a1}}\left(h\sqrt{D_{H_2CO_3}k_d}\right)=\left[H_2CO_3\right]_h\left(h\sqrt{D_{H_2CO_3}k_d}\right)+D_{HCO_3}\left[HCO_3^-\right]_h$$

$$\left[HCO_3^-\right]_0\left(K_{a1}D_{HCO_3}+\left[H^+\right]_0\left(h\sqrt{D_{H_2CO_3}k_d}\right)\right)=K_{a1}\left(\left[H_2CO_3\right]_h\left(h\sqrt{D_{H_2CO_3}k_d}\right)+D_{HCO_3}\left[HCO_3^-\right]_h\right)$$

$$\left[HCO_3^-\right]_0=\frac{K_{a1}\left(\left[H_2CO_3\right]_h\left(h\sqrt{D_{H_2CO_3}k_d}\right)+D_{HCO_3}\left[HCO_3^-\right]_h\right)}{\left(K_{a1}D_{HCO_3}+\left[H^+\right]_0\left(h\sqrt{D_{H_2CO_3}k_d}\right)\right)}$$

The above equation can be inserted into Eq. (A31) where electric neutrality is assumed in the diffusion layer.

$$D_H\frac{\left([H^+]_h-[H^+]_0\right)}{h}=D_{OH}\frac{\left([OH^-]_h-[OH^-]_0\right)}{h}+D_A\frac{\left([A^-]_h-[A^-]_0\right)}{h}+\frac{D_{HCO_3}}{h}\left(\left[HCO_3^-\right]_h-\left(\frac{K_{a1}\left(\left[H_2CO_3\right]_h\left(h\sqrt{D_{H_2CO_3}k_d}\right)+D_{HCO_3}\left[HCO_3^-\right]_h\right)}{\left(K_{a1}D_{HCO_3}+\left[H^+\right]_0\left(h\sqrt{D_{H_2CO_3}k_d}\right)\right)}\right)\right) \quad \text{(A31b)}$$

The chemical equilibrium in Eqs. (A1) and (A2) was used to define all of the species at the surface of the tablet ($x = 0$) in either terms of $\left[H^+\right]_0$ or $\left[HA\right]_0$.

$$D_H\frac{\left([H^+]_h-[H^+]_0\right)}{h}=\frac{D_{OH}}{h}\left([OH^-]_h-\frac{K_w}{[H^+]_0}\right)+\frac{D_A}{h}\left([A^-]_h-\frac{[HA]_0K_a^A}{[H^+]_0}\right)+\frac{D_{HCO_3}}{h}\left(\left[HCO_3^-\right]_h-\left(\frac{K_{a1}\left(\left[H_2CO_3\right]_h\left(h\sqrt{D_{H_2CO_3}k_d}\right)+D_{HCO_3}\left[HCO_3^-\right]_h\right)}{\left(K_{a1}D_{HCO_3}+\left[H^+\right]_0\left(h\sqrt{D_{H_2CO_3}k_d}\right)\right)}\right)\right) \quad \text{(A31c)}$$

The pH at the surface can be calculated by applying the boundary conditions to equation (31C).

Boundary conditions at $X = h$ (bulk solution):

$$\left[HA\right]=\left[HA\right]_h\cong 0$$

$$\left[A^-\right]=\left[A^-\right]_h\cong 0$$

$$\left[H^+\right]=\left[H^+\right]_h\,(\text{known})=\text{bulk pH}$$

$$\left[OH^-\right]=\left[OH^-\right]_h\,(\text{known})$$
$$=\text{known based on bulk pH and chemical equilibrium}$$

$$\left[HCO_3^-\right]=\left[HCO_3^-\right]_h\,(\text{known})=\text{experimental buffer concentration}$$

$$\left[H_2CO_3\right]=\left[H_2CO_3\right]_h\,(\text{known})=\text{experimental buffer concentration}$$

$$\left[CO_2\right]=\left[CO_2\right]_h\,(\text{known})=\text{analyzed with a } CO_2 \text{ monitor}$$

Boundary conditions at $X = 0$ (surface of the drug):

$$\left[HA\right]=\left[HA\right]_0\,(\textit{Weak acid intrinsic Solubility})$$

$$\left[A^-\right]=\left[A^-\right]_0\,(\text{unknown})$$

$$\left[H^+\right]=\left[H^+\right]_0\,(\text{unknown})$$

$$\left[OH^-\right]=\left[OH^-\right]_0\,(\text{unknown})$$

$$\left[HCO_3^-\right]=\left[HCO_3^-\right]_0\,(\text{unknown})$$

$$\left[H_2CO_3\right]=\left[H_2CO_3\right]_0\,(\text{unknown})$$

$$[CO_2] = [CO_2]_0 \text{ (unknown)}$$

$$D_H \frac{([H^+]_h - [H^+]_0)}{h} = \frac{D_{OH}}{h}\left([OH^-]_h - \frac{K_w}{[H^+]_0}\right) + \frac{D_A}{h}\left(-\frac{[HA]_0 K_a^A)}{[H^+]_0}\right) + \frac{D_{HCO_3}}{h}\left([HCO_3^-]_h - \left(\frac{K_{a1}\left([H_2CO_3]_h\left(h\sqrt{D_{H_2CO_3}k_d}\right) + D_{HCO_3}[HCO_3^-]_h\right)}{\left(K_{a1}D_{HCO_3} + [H^+]_0\left(h\sqrt{D_{H_2CO_3}k_d}\right)\right)}\right)\right) \quad \text{(A31d)}$$

Multiplying Eq. (A31d) by h and subtracting the left side of the equation from the right side results in the following cubic equation to solve for $[H^+]_0$.

$$p[H^+]_0^3 + q[H^+]_0^2 + r[H^+]_0 + s = 0 \quad \text{(A34)}$$

$$\boldsymbol{p} = D_H\left(h\sqrt{D_{H_2CO_3}K_d}\right)$$

$$\boldsymbol{q} = -D_H[H^+]_h\left(h\sqrt{D_{H_2CO_3}K_d}\right) + D_{OH}[OH^-]_h\left(h\sqrt{D_{H_2CO_3}K_d}\right) + D_{HCO_3}[HCO_3^-]_h\left(h\sqrt{D_{H_2CO_3}K_d}\right) + K_{a1}D_{HCO_3}D_H$$

$$\boldsymbol{r} = -K_{a1}D_{HCO_3}D_H[H^+]_h + K_{a1}D_{HCO_3}D_{OH}[OH^-]_h - D_{OH}K_w\left(h\sqrt{D_{H_2CO_3}K_d}\right) - D_A[HA]_0K_a^A\left(h\sqrt{D_{H_2CO_3}K_d}\right) - D_{HCO_3}^2K_{a1}[HCO_3^-]_h - D_{HCO_3}[H_2CO_3]_hK_{a1}\left(h\sqrt{D_{H_2CO_3}K_d}\right) + D_{HCO_3}^2K_{a1}[HCO_3^-]_h$$

$$\boldsymbol{s} = -K_{a1}D_{HCO_3}D_{OH}K_w - K_{a1}D_{HCO_3}D_A[HA]_0K_a^A$$

The total drug flux is dependent on the interfacial pH.

$$D_{HA}\frac{([HA]_h - [HA]_0)}{h} + D_A\frac{([A^-]_h - [A^-]_0)}{h} = \text{total drug flux} \quad \text{(A35a)}$$

$$[HA] = [HA]_h \cong 0$$

$$[A^-] = [A^-]_h \cong 0$$

$$D_{HA}\frac{-[HA]_0}{h} + D_A\frac{-[A^-]_0}{h} = \text{total drug flux} \quad \text{(A35b)}$$

$$D_{HA}\frac{-[HA]_0}{h} - \frac{D_A}{h}\frac{[HA]_0K_a^A}{[H^+]_0} = \text{total drug flux} \quad \text{(A35c)}$$

Assuming the diffusion coefficient of the ionized form of the drug is equal to the unionized form of the drug simplifies Eq. (35c) to Eq. (35d).

$$-D_{HA}\frac{[HA]_0}{h}\left(1 + \frac{K_a^A}{[H^+]_0}\right) = \text{total drug flux} \quad \text{(A35d)}$$

REFERENCES

1. Mooney K, Mintun M, Himmelstein K, Stella V. 1981. Dissolution kinetics of carboxylic acids II: Effect of buffers. J Pharm Sci 70(1):22–32.

2. Amidon GL, Lennernas H, Shah VP, Crison JR. 1995. A theoretical basis for a biopharmaceutic drug classification: The correlation of in vitro drug product dissolution and in vivo bioavailability. Pharm Res 12(3):413–420.

3. Aunins JG, Southard MZ, Myers RA, Himmelstein KJ, Stella VJ. 1985. Dissolution of carboxylic acids III. The effect of polyionizable buffers. J Pharm Sci 74(12):1305–1316.

4. McNamara DP, Amidon GL. 1988. Reaction plane approach for estimating the effects of buffers on the dissolution rate of acidic drugs. J Pharm Sci 77(6):511–517.

5. Sheng JJ, McNamara DP, Amidon GL. 2009. Toward an in vivo dissolution methodology: A comparison of phosphate and bicarbonate buffers. Mol Pharm 6(1):29–39.

6. Neervannan S, Southard MZ, Stella VJ. 2012. Dissolution of weak acids under laminar flow and rotating disk hydrodynamic conditions: Application of a comprehensive convective-diffusion-migration-reaction transport model. J Pharm Sci 101(9):3180–3189.

7. Jacobs MH, Stewart DR. 1942. The role of carbonic anhydrase in certain ionic exchanges involving the erythrocyte. J General Physiol 13:539–552.

8. Kaunitz JD, Akiba Y. 2006. Duodenal carbonic anhydrase: Mucosal protection, luminal chemosensing, and gastric acid disposal. Keio J Med 55(3):96–106.

9. Kaunitz JD, Akiba Y. 2007. Review article: Duodenal bicarbonate–mucosal protection, luminal chemosensing and acid–base balance. Aliment Pharmacol Ther 24:169–176.

10. McNamara DP, Whitney KM, Goss SL. 2003. Use of a physiologic bicarbonate buffer system for dissolution characterization of ionizable drugs. Pharm Res 20(10):1641–1646.

11. Hogan DL, Ainsworth MA, Isenberg JI. 1994. Review article: Gastroduodenal bicarbonate secretion. Aliment Pharmacol Ther 8:475–488.

12. Sjoblom M. 2011. Duodenal epithelial sensing of luminal acid: Role of carbonic anhydrases. Acta Physiol 201:85–95.

13. Brinkman A, Glasbrenner B, Vlatten A, Eberhardt H, Geldner G, Radermacher P, Georgieff M, Weideck H. 2001. Does gastric juice ph influence tonometric PCO_2 measured by automated air tonometry. Am J Respir Crit Care Med 163:1150–1152.

14. McGee LC, Hastings AB. 1942. The carbon dioxide tension and acid-base balance of jejunal secretions in man. J Biol Chem 142:893–904.

15. Rune S. 1972. Acid–base parameters of duodenal contents in man. Gastroenterology 62:533–539.

16. Kivela A, Kivela J, Saarnio J, Parkkila S. 2005. Carbonic anhydrase in normal gastrointestinal tract and gastrointestinal tract and gastrointestinal tumours. World J Gastroenterol 11(2):155–163.

17. Boni JE, Brickl RS, Dressman J. 2007. Is bicarbonate buffer suitable as a dissolution medium? J Pharm Pharmacol 59(10):1375–1382.

18. Fadda HM, Merchant HA, Arafat BT, Basit AW. 2009. Physiological bicarbonate buffers: Stabilisation and use as dissolution media for modified release systems. Int J Pharm 382(1–2):56–60.

19. Garbacz G, Kolodziej B, Koziolek M, Weitschies W, Klein S. 2014. A dynamic system for the simulation of the fasting luminal pH-gradients using hydroden carbonate buffers for dissolution testing of ionisable compounds. Eur J Pharm Sci 51:224–231.

20. Wallin M, Bjerle I. 1989. A mass transfer model for limestone dissolution from a rotating cylinder. Chem Eng Sci 44(1):61–67.
21. Dreybrodt W, Buhmann D. 1991. A mass transfer model for dissolution and precipitation of calcite from solutions in turbulent motion. Chem Geol 90:107–122.
22. Dreybrodt W, Lauckner J, Zaihua L, Svensson U, Buhmann D. 1996. The kinetics of the reaction $CO_2 + H_2O \rightarrow H^+ HCO_3^-$ as one of the rate limiting steps for the dissolution of clacite in the system H_2O-CO_2-$CaCO_3$. Geochim Cosmochim Acta 60(18):3375–3381.
23. Liu Z, Dreybrodt W. 1997. Dissolution kinetics of calcium carbonate minerals in H_2O-CO_2 solutions in turbulent flow: The role of the diffusion boundary layer and the slow reaction $H_2O + CO_2 = H^+ + HCO_3^-$. Geochim Cosmochim Acta 61(14):2879–2889.
24. Kaufmann G, Dreybrodt W. 2007. Calcite dissolution kinetics in the system $CaCO_3$-H_2O-CO_2 at high undersaturation. Geochim Cosmochim Acta 71:1398–1410.
25. Butler JN. 1991. Carbon dioxide equilibria and their applications. Reading, Mass: Addison-Wesley.
26. Harned HS, Davis Jr R. 1943. The Ionization Constant of Carbonic Acid in Water and the Solubility of Carbon Dioxide in Water and Aqueous Salt Solutions from 0 to 50 deg C. Journal of the American Chemical Society 65:2030–2037.
27. Roughton FJW. 1935. Recent Work on Carbon Dioxide Transport By the Blood. Physiol Rev 15:241–296.
28. Mills GA, Urey HC. 1940. The Kinetics of Isotopic Exchange Between Carbon Dioxide, Bicarbonate Ion, Carbonate Ion and Water. J Am Chem Soc 62:1019–1026.
29. Pinsent BRW, Pearson L, Roughton FJW. 1956. The Kinetics of Combination of Carbon Dioxide With Hydroxide Ions. Trans Faraday Soc 15:1594–1598.
30. Garg LS, Maren TH. 1972. The Rates of Hydration of Carbon Dioxide and Dehydration of Carbonic Acid At 37°. Biochim Biophys Acta 261:70–76.
31. Soli AL, Byrne RH. 2002. Carbon Dioxide System Hydration and Dehydration Kinetics and the Equilibrium CO2/H2CO3 Ratio in Aqueous NaCl Solution. Marine Chemistry 78:65–73.
32. Roughton FJW 1941. 1941. The Kinetics and Rapid Thermochemistry of Carbonic Acid. J Biol Chem 129:2930–2934.
33. Berger RL, Stoddart LC. 1965. Combined Calorimeter and Spetrophotometer for Observing Biological Reactions. The Review of Scientific Instruments 36:78–84.
34. Rossi-Bernardi L, Berger RL. 1968r. he Rapid Measurement of pH by the Glass Electrode: The Kinetics of Dehydration of Carbonic Acid at 25º and 37º. The Journal of Biological Chemistry 243:1297–1302.
35. M M EIGEN, GG G G HAMMES (1963) ELEMENTARY STEPS IN ENZYME REACTIONS (AS STUDIED BY RELAXATION SPECTROMETRY). Advances in enzymology and related areas of molecular biology 25: 1–38 [PubMed].
36. Nassanen R. 1947. Potentiometric Study on the First Ionization of Carbonic Acid in Aqueous Solutions of Sodium Chloride. Acta Chemica Scandinavica 1:204–209.
37. Wissbrun KF, French DM. 1954. The True Ionization Constant of Carbonic Acid in Aqueous Solution from 5º to 45º. J Phys Chem 58:693–695.
38. Harned HS, Bonner FT. 1945. The First Ionization of Carbonic Acid in Aqueous Solutions of Sodium Chloride. J Am Chem Soc 67:1026–1031.
39. Magid E, Turbeck BO. 1968. The Rates of the Spontaneous Hydration of CO2 and the Reciprocal Reaction in Neutral Aqueous Solutions Between 0º and 38º. Biochim ET Biophys Acta 165:515–524.
40. Mooney KG, Mintun M, Himmelstein K, Stella V. 1981. Dissolution kinetics of carboxylic acids I: Effect of pH under unbuffered conditions. J Pharm Sci 70(1):13–22.
41. Levich VG. 1962. Physicochemical hydrodynamics. New jersey: Prentice Hall.
42. Grijseels H, Crommelin DJA, Blaey CJD. 1981. Hydrodynamic approach to dissolution rate. Pharm Weekbl (Scientific Edition) 3:129–144.
43. Mooney KG, Rodriguez-Gaxiola M, Mintun M, Himmelstein KJ, Stella VJ. 1981. Dissolution kinetics of phenylbutazone. J Pharm Sci 70(12):1358–1365.
44. Karl AL, Majella EL, Corrigan OI. 2003. Effect of buffer media composition on the solubility and effective permeability coefficient of ibuprofen. Int J Pharm 253:49–59.
45. Fagerberg J, Tsinman O, Sun N, Tsinman K, Avdeef A, Bergstrom C. 2010. Dissolution Rate and Apparent Solubility of Poorly Soluble Drugs in Biorelevant Dissolution Media. Molecular Pharmaceutics 7:1419–1430.
46. Tsinman K, Avdeef A, Tsinman O, Voloboy. 2009. Powder Dissolution Method for Estimating Rotating Disk Intrinsic Dissolution Rates of Low Solubility Drugs. Pharmaceutical Research 26:2093–2100.
47. Avdeef A, Tsinman O. 2008. Miniaturized Rotating Disk Intrinsic Dissolution Rate Measurement: Effects of Buffer Capacity in Comparisons to Traditional Wood's Apparatus. Pharmaceutical Research 25:2613–2627.
48. Zeebe RE. 2011. On the molecular diffusion coefficients of dissolved CO2, HCO3-, and CO32- and their dependence on isotopic mass. Geochimica et Cosmochimica Acta 75:2483–2498.
49. Frank MJW, Kuipers JAM, Swaaij WPMv. 1996. Diffusion Coefficients and Viscosities of CO2 + H2O, CO2 + CH3OH, NH3 + H2O, and NH3 + CH3OH Liquid Mixtures. J Chem Eng Data 41: 297–302.
50. Guo D, Thee H, Silva Gd, Chen J, Fei W, Kentish S, Stevens GW. 2011. Borate-catalyzed carbon dioxide hydration via the carbonic anhydrase mechanism. Environ Sci Technol 45:4802–4807.